Photoactuated Droplet Microfluidics

by

Ryan T. Frederick

A PROJECT

submitted to

Oregon State University

University Honors College

in partial fulfillment of
the requirements for the
degree of

Honors Baccalaureate of Science in Chemical Engineering (Honors Scholar)

Presented May 16, 2011
Commencement June 11, 2011

AN ABSTRACT OF THE THESIS OF

Ryan T. Frederick for the degree of Honors Baccalaureate of Science in Chemical Engineering presented on May 16, 2011. Title: Photoactuated Droplet Microfluidics

Abstract Approved: _____

Vincent T. Remcho

A system of Photoactuated Droplet Microfluidics (PDM), in which a droplet of fluid is moved by way of the manipulation of the wettability of a spiropyran functionalized surface via irradiation with ultraviolet and visible light, was proposed. The photochromic behaviors of several species of spiropyran were studied and a procedure was prepared for testing the photochromism of spiropyran species synthesized in lab. Two methods were proposed to optimize the surface area of spiropyran functionalized polymer available to a droplet in the PDM system. The first method was the physical modification of PMMA to created posted structures through the use of a laser machining and hot embossing process. The second method involved the construction and optimization of an electrospinner, which was used to create PMMA nanofibers functionalized with spiropyran. The following describes the successful proof of photoswitchable wettability in the physically modified chips, and photochromism in the electrospun nanofibers, and describes the significance of these findings towards the development of a PDM system.

Key Words: photochromism, photoactuation, spiropyran, photoswitching, microfluidics, droplet microfluidics, digital microfluidics, photoactuated droplet microfluidics, PDM, electrospinning, electrospinner

Corresponding E-mail Address: frederir@onid.orst.edu

Photoactuated Droplet Microfluidics

by

Ryan T. Frederick

A PROJECT

submitted to

Oregon State University

University Honors College

in partial fulfillment of
the requirements for the
degree of

Honors Baccalaureate of Science in Chemical Engineering (Honors Scholar)

Presented May 16, 2011
Commencement June 11, 2011

Honors Baccalaureate of Science in Chemical Engineering project of Ryan T. Frederick presented on May 16, 2011.

APPROVED:

Mentor, representing Chemistry

Committee Member, representing Chemical Engineering

Committee Member, representing Chemistry

Chair, Department of Chemical Engineering

Dean, University Honors College

I understand that my project will become part of the permanent collection of Oregon State University, University Honors College. My signature below authorizes release of my project to any reader upon request.

Ryan T. Frederick, Author

ACKNOWLEDGEMENTS

I would like to thank…

My mentor, Dr. Vincent T. Remcho, for being so generous and accommodating in the opportunities he gave to me.

Dr. Goran Jovanovic for his support as a committee member as well as for being a supportive advisor throughout my undergraduate career in the Chemical Engineering department.

Dr. Myra Koesdjojo for providing so much assistance as a committee member and friend as I found my way through this project.

Dr. Jintana Nammoonnoy (Dao) for being such a brilliant resource as I explored this interesting topic.

Dr. Jack T. Rundel for being so knowledgeable, patient, and friendly when it came to the many hours of machining, embossing, and metrology required in this project.

Brian Fuchs for his perseverance in the construction and optimization of the electrospinner, as well as his continued friendship throughout my time at OSU.

Beth Dunfield for her collaboration in the photochromism experiments and for her constant kindness.

Patrick Ramsing for his assistance in the construction of the electrospinner and his friendship for the past several years.

Mark Warner for all of his assistance in understanding and assembling components of the PDM project related to electricity.

All additional members of the Remcho research team I encountered during my year spent doing research, Adeniyi Adenuga, Esha Chatterjee, Chris Heist, Tae-Hyeong Kim, Saki Kondo, Yu Chu Lin (Zoe), Natalia Pylypiuk, and Yuanyuan Wu (YY), for being friendly and inspirational colleagues.

My professors at Oregon State University for instilling within me many of the skills needed to work on this project.

My friends and family for their unending support.

And my parents, above all others, for always going above and beyond in terms of their love and support.

CONTRIBUTION OF AUTHORS

Dr. Vincent Remcho and Dr. Myra Koesdjojo edited all chapters of this thesis and collaborated on all research and material included. Beth Dunfield collaborated on procedure and research in Chapter One. Dr. Jack T. Rundel collaborated on all fabrication procedures in Chapter Two, and all fabrication was done at the Microproducts Breakthrough Institute. Dr. Jintana Nammoonnoy collaborated on the spiropyran functionalization procedures in Chapter Two. Patrick Ramsing and Brian Fuchs collaborated on the design and construction of the electrospinner in Chapter Three. Brian Fuchs additionally collaborated on all optimization work related to the electrospinner in Chapter Three.

TABLE OF CONTENTS

LIST OF FIGURES

LIST OF TABLES

LIST OF APPENDICES

LIST OF APPENDIX TABLES

Introduction

The proposed system, a photoactuated droplet microfluidics system, is a method of manipulating droplets of liquid through the use of molecules with photoswitchable wettability.

Chapter 1 is an introduction to the concept of photochromism and spiropyran molecules. Tests were conducted to better understand photochromism in several species of spiropyrans, and a method of "polymer disc" experiments were developed into an experimental procedure that could be later used to determine the photochromism of spiropyrans synthesized in-lab.

Chapter 2 describes a path towards the development of a photoactuated droplet microfluidics system using spiropyran molecules directly functionalized on a physically modified surface. The methods of creating the physical system of posted and functionalizing the posts with spiropyran, as well as the results of these tests, are described.

Chapter 3 describes a secondary path towards the development of a photoactuated droplet microfluidics system through the creation of spiropyran-functionalized nanofibers. The construction and optimization of an electrospinning device are thoroughly described, and it is proven that the device creates photochromic nanofibers.

Through the description of two paths towards creating photoswitchable surfaces, it is proven that photoactuated wettability changes are possible, and implied that a photoactuated droplet microfluidics system would be viable.

Chapter 1: Spiropyrans and Photochromism

1.1 Introduction and Background

Photochromic species such as spiropyrans and azobenzene provide a way of changing a molecule's color, wettability, and other physical properties using only ultraviolet and monochromic visible light. These were previously utilized in the Remcho lab group in Dr. Jintana Nammoonnoy's dissertation, *Photoactivable Microfluidic Device for Heavy Metal Ion Extraction* as a means of filtration for extracting heavy metals from a solution. This led the group to maintain curiosity about these molecules, and prompted questions about their possible use for wettability switching applications and additional methods of functionalization, such as electrospinning. An experimental review of photochromism was undertaken and methods for detecting photochromic switching were developed in order to have a method for detecting photochromism in species of spiropyran developed in-lab.

1.1.1 Photochromism

Photochromic species are those which undergo a reversible transformation between forms when exposed to electromagnetic radiation. Each isomeric form is characterized by a different light absorption region (wavelength), which causes a color change in the species itself. Switching between forms will also bring about changes in other properties, such as wettability. A notable photochromic species are the spiropyrans and spirooxazzines, which convert from their standard (SP) form to the planar merocyanine (MC) form in the presence of UV light by way of an electrocyclic ring opening reaction. Irradiation with visible light switched the spriopyran back to its original

(SP) form. Another species of note is azobenzene, which transitions between trans and cis isomers in the presence of UV light.

The discovery of photochromism came in 1919 when J. Lifschitz and C. L. Joffe discovered that colorless dye-derivatives would gain color through exposure to UV irradiation (*1*),(*2*). The concept of thermochromism was discovered at roughly the same time when it was found that di-β-naphthospiran is blue-violet when heated but loses its color when cooled. This compound was the subject of three reports published within a short time-span in 1926 (*3*). After this discovery research into thermochromism took off, and led inevitably into an increase in photochromism research.

It was noted early on in photochromism research that, based on the molar extinction coefficient calculated after both thermochromic and photochromic changes, the changes due to heat or UV irradiation were likely the same (*4*). In fact, the changes due to thermochromism and the changes due to photochromism resulted in states that were the same spectral color (*2*). Furthermore, UV irradiation seemed to be very effective, causing essentially complete conversion. It was also noted that the photochromic change was reversible, solutions lost their color when not in the presence of UV irradiation, and the reversal was noted to have a temperature dependence, with an increased rate of reversal at higher temperatures (*4*). Even at relatively stable temperatures, the reversal could be prompted by irradiation with visible light (*2*). The actual molecular mechanism of switching depends on the molecule being switched.

There are a variety of applications for photochromic compounds. One category of applications takes advantage of the changes in chromism, such as optical information storage, authentication systems, cosmetics, and glasses that transition into sunglasses.

Another category of applications, all being explored more recently, takes advantage of the other changes that occur during switching such as changing refractive index, electric conductivity, phase transitions, solubility, viscosity, and surface wettability.

1.1.2 Spiropyrans

Spiropyran molecules are characterized by two heterocyclic parts linked via a tetrahedral sp^3 spiro carbon atom. See Figure 1.

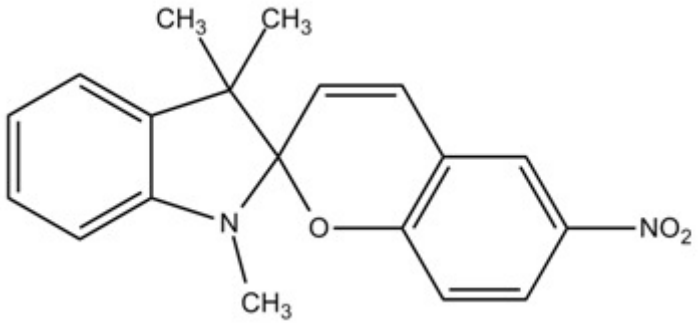

Figure 1: An example of a spiropyran molecule, this is the structure for 1′,3′-Dihydro-1′,3′,3′-trimethyl-6-nitrospiro[2H-1-benzopyran-2,2′-(2H)-indole].

As was noted previously, photochromism as a concept was first discovered by J. Lifschitz and C. L. Joffe in 1919 in some dye-derivatives. The compounds known as spiropyrans were discovered to be thermochromic around 1951 in research done by C.F. Koelsch and in research done by E.B. Knott (*4*). The photochromic nature of spiropyrans was discovered in 1951 in research published by Chaudé and Rumpf and in research published by Fischer and Hirshberg (*4*). As can be seen in Figure 2, the mechanism for the switching in the presence of UV light involves a ring-opening at the carbon-oxygen bond (*5*). This open form is called merocyanine (MC), and produces vivid color. In the presence of visible light, the molecule reverts to the original (SP) form (*5*). A typical

range for UV switching is near 366 nm, and a typical range for visible light is 500 nm - 550 nm (*6*).

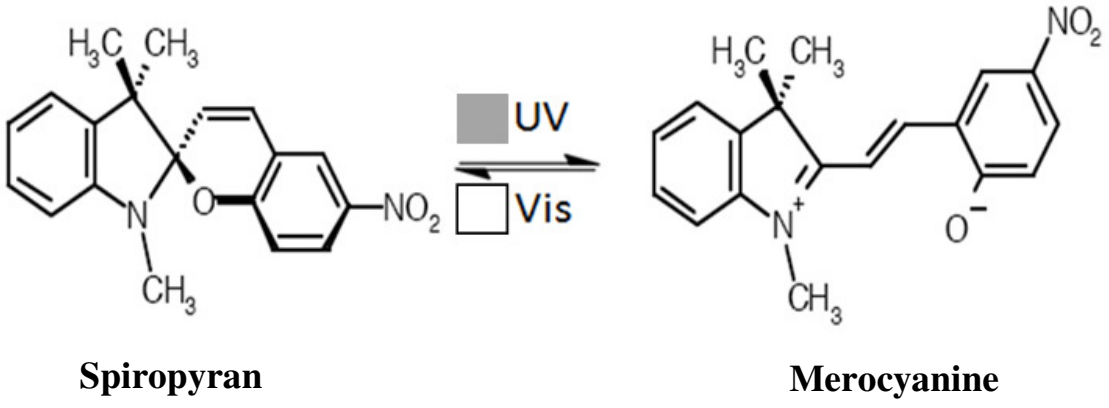

Figure 2: The transition from spiropyran state to merocyanine state in the presence of UV light, and the reverse in visible light, for 1′,3′-Dihydro-1′,3′,3′-trimethyl-6-nitrospiro[2H-1-benzopyran-2,2′-(2H)-indole]. (*7*).

Hirshberg went on to study spiropyran molecules in depth and reported on his discovery of three spiropyrans and a bianthrone derivative that could be switched with ultraviolet and monochromatic visible light. The effect of lights on different the four compounds in various media was extensively studied, and Hirshberg proposed the use of this molecule for a photochemical memory model (*2*).

One application that was explored recently, and has been alluded to already, is Dr. Jintana Nammoonnoy's research into the use of spiropyrans for heavy metal ion extraction. It was demonstrated that spiropyrans immobilized on poly(methylmethacrylate), PMMA, microchips would take up metal irons in the presence of UV irradiation (during the SP to MC transition). It was also demonstrated that this could be reversed in the presence of visible light.

1.1.3 Azobenzene

Azobenzene switches from its trans-isomer form to cis-isomer form in the presence of UV irradiation, and this reverses in the presence of visible light, Figure 3. Previous values for azobenzene switching are at a UV irradiation of 365 nm and in visible light at around 494 nm (*6*).

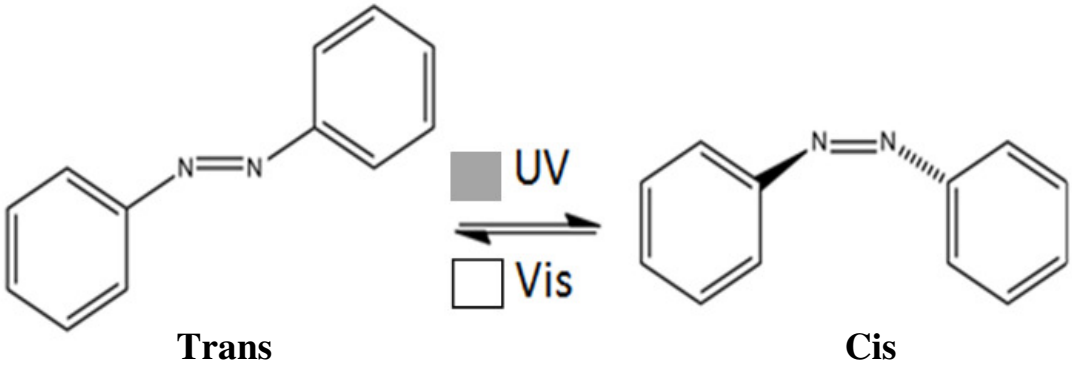

Figure 3: The transition from trans-isomer to cis-isomer of azobenzene in the presence of UV light, and the reverse in visible light.

1.2 Materials and Methods

1.2.1 Solution Tests

In order to understand the photochromic nature of several species of spiropyrans and compare them, preliminary testing was done on the exposure of spiropyran solutions in clear glass vials to UV and visible light. A class II ($p<50mW$) 405 nm laser pointer, a 365 nm long wave UV lamp (Spectronics Corp. model X-15A), an Aries – 75 class IIIb ($75\ mW<p<205\ mW$) 532 nm laser module, and Glendale Protective Technologies laser safety goggles were employed in these tests.

A solution of 1.5 mg spiropyran to 1 mL chloroform was used. All spiropyran species were from Sigma-Aldrich®. The species that, for the purpose of these

experiments, was referred to as Species #1 is 1′,3′-Dihydro-1′,3′,3′-trimethyl-6-nitrospiro[2H-1-benzopyran-2,2′-(2H)-indole], which was identified by C.A.S. number 1498-88-0, formula $C_{19}H_{18}N_2O_3$, and had a formula weight of 322.36 . Species #2 was 1′,3′-Dihydro-8-methoxy-1′,3′,3′-trimethyl-6-nitrospiro[2H-1-benzopyran-2,2′-(2H)-indole], which was identified by C.A.S. number 1498-89-1, formula $C_{20}H_{20}N_2O_4$, and formula weight 352.38 g/mol. Species #3 was 5-Chloro-1,3-dihydro-1,3,3-trimethylspiro[2H-indole-2,3′-(3H)naphth[2,1-b](1,4)oxazine], which was identified by the C.A.S. number 27333-50-2, formula $C_{22}H_{19}ClN_2O$, and has a formula weight of 362.85 g/mol. Species 4 from Acros was Spiro[2H-1-benzopyran-2,2'-[2H]indol]-6-ol,1',3'-dihydro-1',3',3'-trimethyl- which had a C.A.S. number of 23001-29-8, a formula of $C_{19}H_{19}NO_2$, and a formula weight of 293.36 g/mol. The molecular structure for all of these can be found as Figure 4.

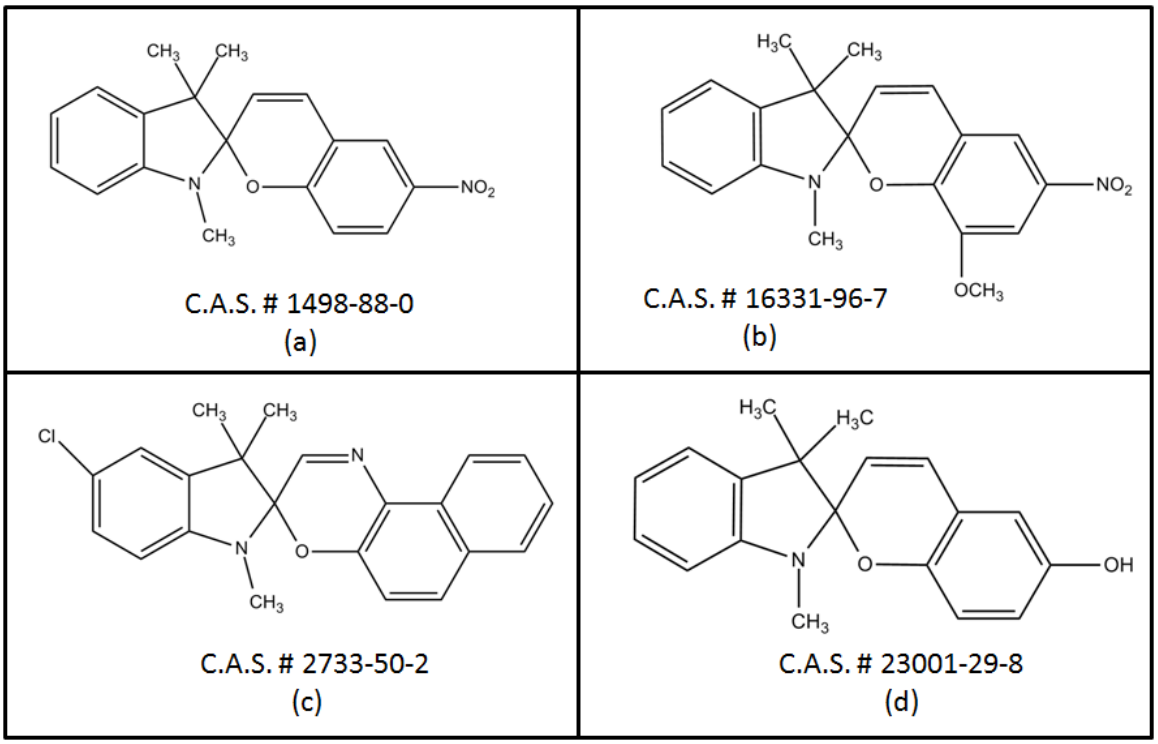

Figure 4: (a) The molecular structure of spiropyran "Species #1." (b) The molecular structure of spiropyran "Species #2." (c) The molecular structure of spirooxazine "Species #3." (d) The molecular structure of spiropyran "Species #4," Images are based on the images adorning the bottles from Sigma Aldrich® (a-c) or Acros® (d).

The first solution experiment was performed on a single concentration (1 mM) of spiropyran species 1, 2, and 3 in chloroform. The first experiment was meant as a qualitative test of both switches (SP to MC and MC to SP) by means of observation of the photochromism. The procedure for solution preparation consisted of making 0.1 molar stock solutions and then creating the sampled from dilutions. Pictures were taken of the three solutions before exposure to UV light, after five minutes of irradiation via UV lamp, and after five minutes of irradiation via the visible laser.

The second solution experiment sought to understand photochromism as a function of species and concentration. Spiropyran species 1, 2, 3, and 4 were prepared in

chloroform. The concentrations prepared depended on how each species performed in the previous experiment, and whether it was thought that a more concentrated or more dilute concentration was required. For species #1, samples A, B, and C comprised 10 mM, 1 mM, and 0.1 mM solutions, respectively. Species #2 samples A, B, and C comprised 1 mM, 0.1 mM, and 0.01 mM solutions, respectively. Species #3 samples A, B, and C comprised 100 mM, 10 mM, and 1 mM solutions, respectively. Species #4 samples A, B, and C comprised 10 mM, 1 mM, and 0.1 mM solutions, respectively. Photos were taken of each set of three concentrations in a species before UV, after five minutes of irradiation via UV lamp, and after five minutes of irradiation via room light. Photos were then taken of each individual concentration in a species after one minute of irradiation via UV lamp and after one minute of irradiation via visible laser.

1.2.2 Disc Experiments

Polymer disc experiments were utilized to better understand the photochromic nature of the spiropyran by highlighting the color changes; it was expected that the thin sheets of dried spiropyran solutions on white backgrounds would yield more easily observable results. Additionally, the disc experiments were meant to check for qualitative signs of wettability, which would only be noticeable if the discs exhibited extreme wettability changes.

The species three and species one 0.1 M stock solutions were utilized as the basis of this experiment. Three separate Sterlitech Corp. polyester membrane filter discs (0.2 μm thickness, 13 mm diameter) had 25 μL droplets of species 1 stock solution added to them. These were labeled discs A, B, and C. Disc A was left in room light for the

duration of the process. Discs B and C were exposed to five minutes of UV light. Finally, disc C was exposed to one minute of the Aries visible laser light shined at the disc's center, then was exposed to one minute of laser light that was moved about the area of the disc. These steps were staggered such that sample B was taken out of the UV lamp as sample C was finished being irradiated with the laser. A 5 μL droplet of water was placed on each of the discs, allowed to wet out, and then pictures were taken. This whole process was repeated for species 3. Then the process was repeated for 0.01 M solutions of both species.

Polymer disc experiments were repeated later without droplets to test the photochromic ability of the silane spiropyran prepared in lab by Dr. Nammoonnoy. This spiropyran is 1'-(3-triethoxysilanpropyl)-3',3'-dimethylspiro[2H,1]benzopyran-2,2'-indoline and can be seen in Figure 5. Three of the Sterlitech Corp. polyester membrane filters were prepared with 1 wt% of the silane spiropyran in a solution of 3:2 DMF:EtOH. Notice that this solution and concentration more closely matched the kind of solutions A 5 μL, 10 μL, and 15 μL droplet of the solution were each placed on separate discs. The Aries laser was used for 1 minute on each of the discs to ensure that the solution was in the SP form. Pictures were taken of each of the discs, and they were exposed to the UV lamp for 15 minutes. Pictures were then taken of the discs.

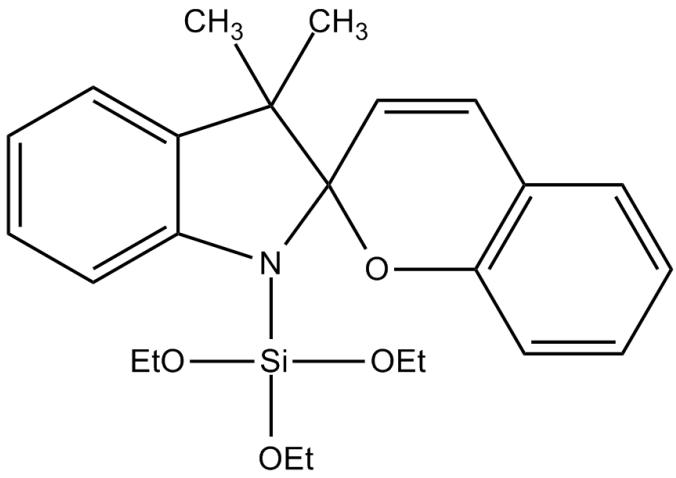

Figure 5: “Silane” Spiropyran, 1’-(3-triethoxysilanpropyl)-3’,3’-dimethylspiro[2H,1]benzopyran-2,2’-indoline.

1.3 Results

1.3.1 Solution Tests

For the first solution experiment, with one concentration of spiropyran in chloroform (0.001 mM) for Species 1, 2, and 3, the following qualitative observations were made. Species #1 was clear before irradiation with UV light. After five minutes of irradiation with the UV lamp the solution became blue-violet. After five minutes of being left in the room’s visible light the solution became a bit lighter. After 45 seconds of irradiation with the visible laser the solution was much lighter. Finally, after an additional minute of irradiation with the laser the solution was essentially clear. Species #2 was blue before exposure to the UV light. The solution remained blue after five minutes of UV irradiation, after five minutes of room visible light, after 45 seconds of laser irradiation, and after an additional minute of laser irradiation. The tint of the solution did not appear to change to a noticeable degree during any of these steps. Species #3 was clear before exposure to UV light. There appeared to be no change after exposure to UV irradiation

and visible irradiation. Records of the solutions that led to these observations may be seen in Figure 6.

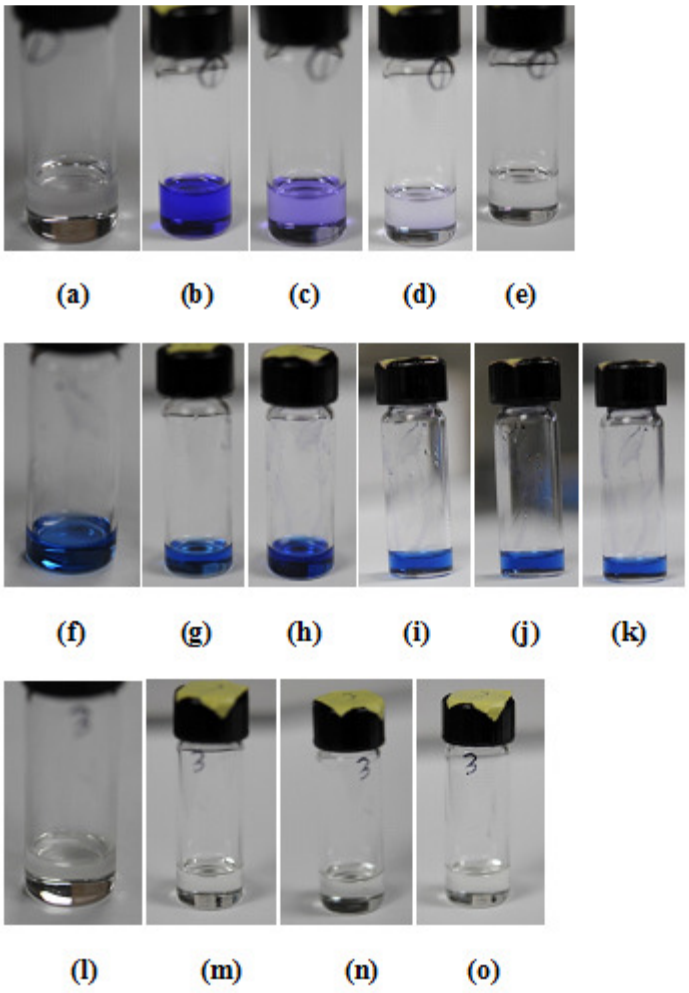

Figure 6: Result of the first solution test for photochromism of all species. The first row shows the transformation in Species 1 (a) before UV irradiation, (b) after five minutes UV lamp irradiation, (c) after five minutes exposure to room light, (d) after 45 seconds exposure to laser (visible light), and (e) after an additional minute of laser exposure. The second row shows how species 2 maintains a constant blue color (f,g) before UV exposure, (h) after UV exposure, (i) after room light exposure, (j) after laser exposure, (k) after laser exposure. The third row shows how Species 3 remains clear (l,m) before UV exposure, (n) after five minutes of UV exposure, and (o) after one minute of laser exposure.

For the second solution experiment, for species #1, the following qualitative observations were made. Sample 1A went from light violet to a relatively dark blue-violet, to violet in the UV/room experiment. In the laser experiment there was a noticeable change from dark blue-violet to light violet in the presence of the visible laser. Sample 1B went from clear to blue-violet, to light violet in the UV/room experiment. In the laser experiment there was a noticeable change from blue-violet to nearly clear in the presence of the visible laser. Sample 1C went from clear to a light blue-violet, to essentially clear in the UV/room experiment. In the laser experiment there was a noticeable change from blue-violet to clear in the presence of the visible laser. The records of the solutions that led to these observations may be seen in Figure 7.

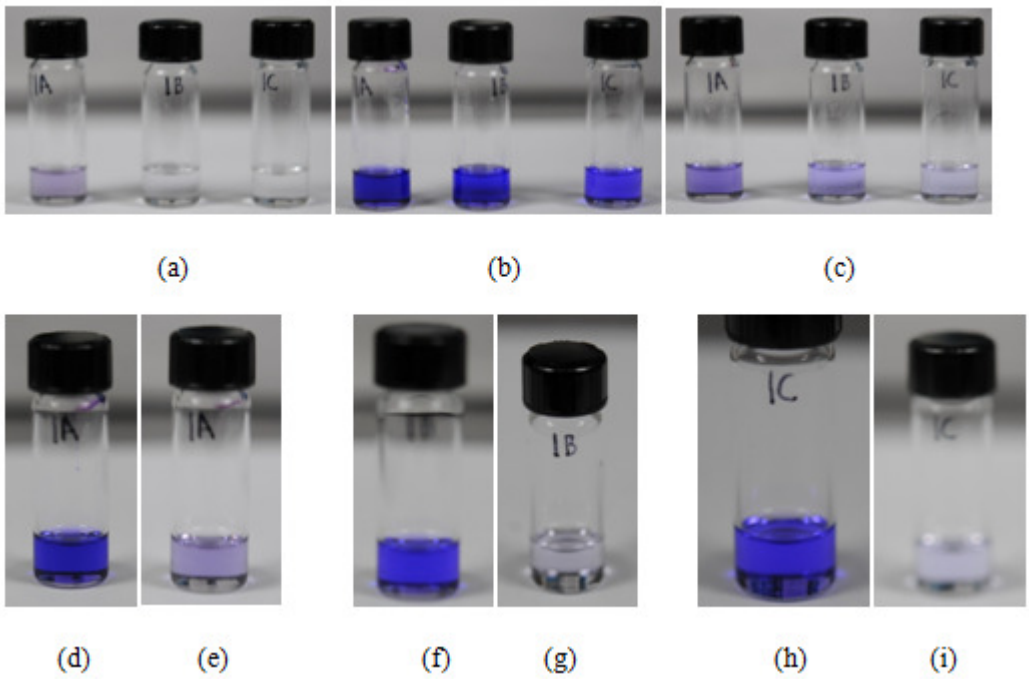

Figure 7: Result of the second solution test for photochromism in species #1. The first row shows the transformation in all three concentrations (a) before UV light, (b) after UV light, and (c) after room light. The second row shows the results of the laser test for a 10 mM solution of species #1 (d) after UV and (e) after laser, the 1 mM solution of species #1 (f) after UV and (g) after laser, and the 0.1 mM solution of species #1 (h) after UV and (i) after laser.

For the second solution experiment, for species #2, the following qualitative observations were made. Sample 2A went from blue to blue (i.e. no noticeable change) to blue (i.e. no noticeable change) in the UV/room experiment. In the laser experiment there was a change from blue to a lighter blue in the presence of the visible laser. Sample 2B went from having a light blue tint to a noticeable light blue and back to having a light tint in the UV/room experiment. In the laser experiment there was a noticeable change from blue to nearly clear in the presence of the visible laser. Sample 2C went from clear to barely blue tinted to clear in the UV/room experiment. In the laser experiment there was a noticeable change from blue tinted to clear. The records of the solutions that led to these observations may be seen in Figure 8.

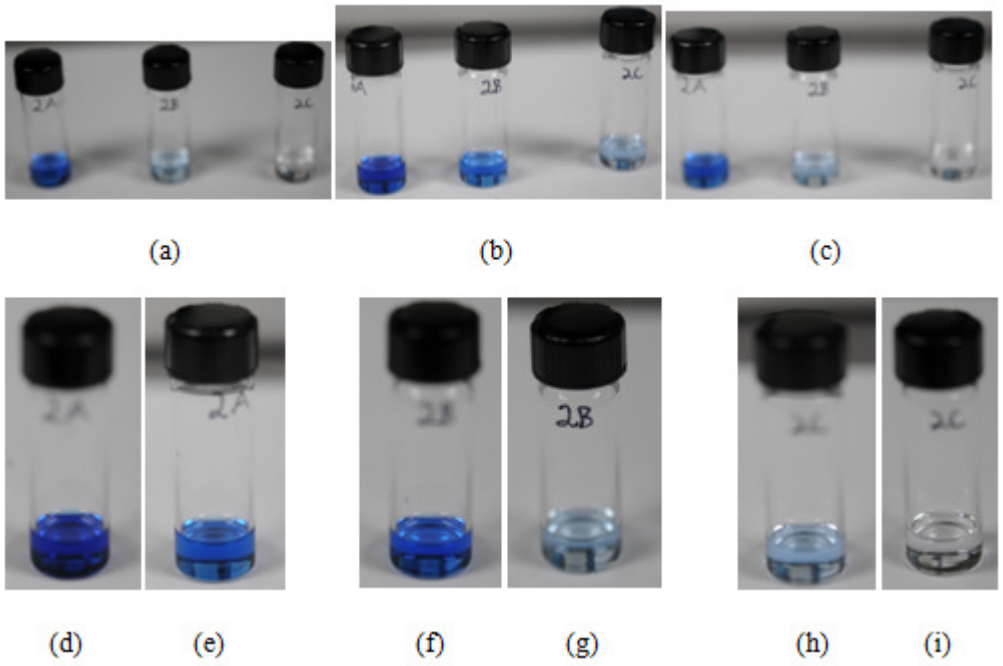

Figure 8: Result of the second solution test for photochromism in species #2. The first row shows the transformation in all three concentrations (a) before UV light, (b) after UV light, and (c) after room light. The second row shows the results of the laser test for a 1 mM solution of species #2 (d) after UV and (e) after laser, the 0.1 mM solution of species #2 (f) after UV and (g) after laser, and the 0.01 mM solution of species #2 (h) after UV and (i) after laser.

For the second solution experiment, for species #3, the following qualitative observations were made. Sample 3A did not change from its dark yellow color during the UV/room experiment and laser experiment. Sample 3B did not change from its slightly yellow tinted color in the UV/room experiment and laser experiment. Sample 3C did not change from clear in the UV/room experiment; the laser experiment was not tried. The records of the solutions that led to these observations may be seen in Figure 9.

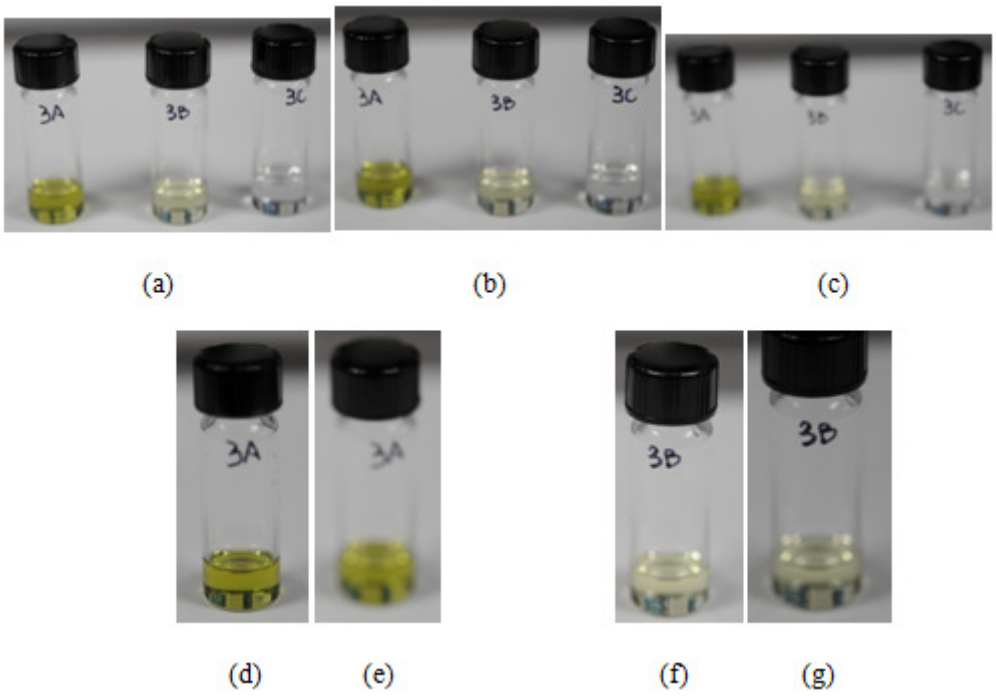

Figure 9: Result of the second solution test for photochromism in species #3. The first row shows the transformation in all three concentrations (a) before UV light, (b) after UV light, and (c) after room light. The second row shows the results of the laser test for a 100 mM solution of species #3 (d) after UV and (e) after laser, and the 10 mM solution of species #3 (f) after UV and (g) after laser. Note that the 1 mM sample was not tried in the laser.

For the second solution experiment, for species #4, the following qualitative observations were made. Sample 3A changed from red to a darker red to having no change in the UV/room experiment. There was a slight change from red to a lighter red in the laser experiment. Sample 3B changed from having a pink tint to a bit darker pink to having no change in the UV/room experiment. There was a slight change from pink to lighter pink in the laser experiment. Sample 3C changed from clear to pink tinted and back to clear in the UV/room experiment. There was a change from slightly tinted to nearly clear in the laser experiment. The records of the solutions that led to these observations may be seen in Figure 10.

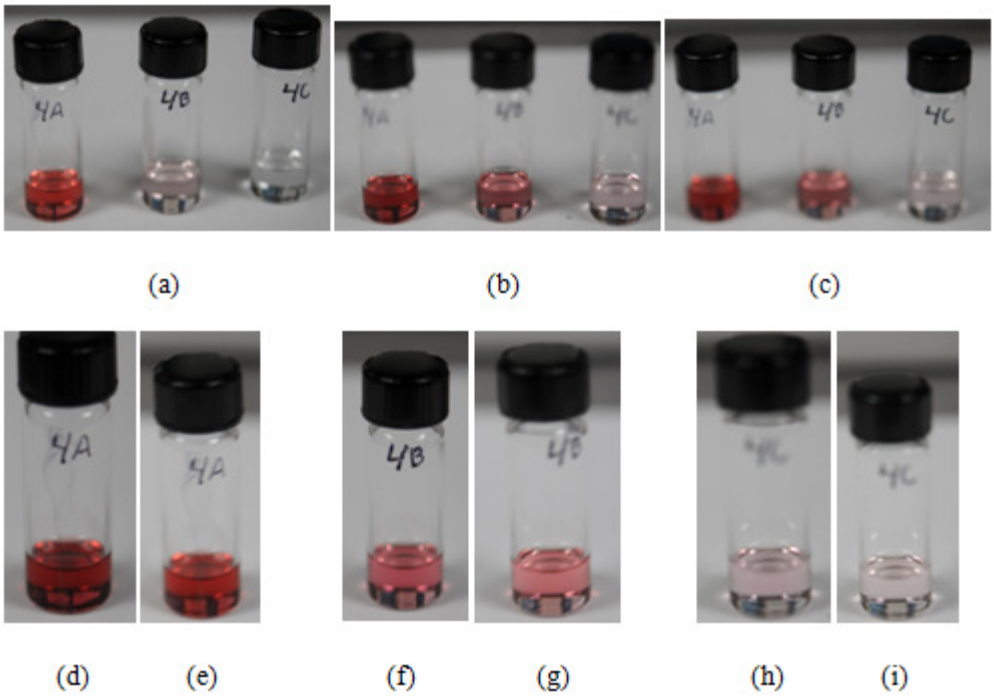

Figure 10: Result of the second solution test for photochromism in species #4. The first row shows the transformation in all three concentrations (a) before UV light, (b) after UV light, and (c) after room light. The second row shows the results of the laser test for a 10 mM solution of species #4 (d) after UV and (e) after laser, the 1 mM solution of species #4 (f) after UV and (g) after laser, and the 0.1 mM solution of species #4 (h) after UV and (i) after laser.

The most useful qualitative results from the polymer disc experiment were the photochromic changes observed. There were no changes in wettability that could be categorized qualitatively, and it was decided that the contact angle be measured quantitatively for electrospun samples later on. For the polymer disc experiments, the qualitative photochromic observations are as follows.

For the 0.1 M stock solution of species 1, there is a noticeable difference between sample A (untreated) – which is an off-white, sample B (only exposed to UV lamp) – which is blue violet, and sample C (exposed to UV and then visible laser) – which is a patchwork of off white, cream, blue, and violet with the visible laser irradiation. There is also a very noticeable difference for the 0.01 M solution of species 1, probably due to the fact that sample A appears whiter at this lower concentration. Sample A is white, sample B is violet, and sample C is again a patchwork with white, off-white, and a noticeable violet spot.

For the 0.1 M stock solution of species 3, there is a less drastic, but still significant, difference between sample A which is off-white/yellow with a slight blue tint, sample B which has a much stronger blue tint, and sample C which is back to white light yellow with only a slight blue tint. In a similar manner to the 0.01 M solution of species 1, sample A of the 0.01 M stock of species 3 starts off considerably whiter. Sample A is white, sample B is noticeably light blue, and sample C has a white spot in the center, but is still pretty close to sample B's appearance.

The results of all of these tests may be viewed in Figure 11.

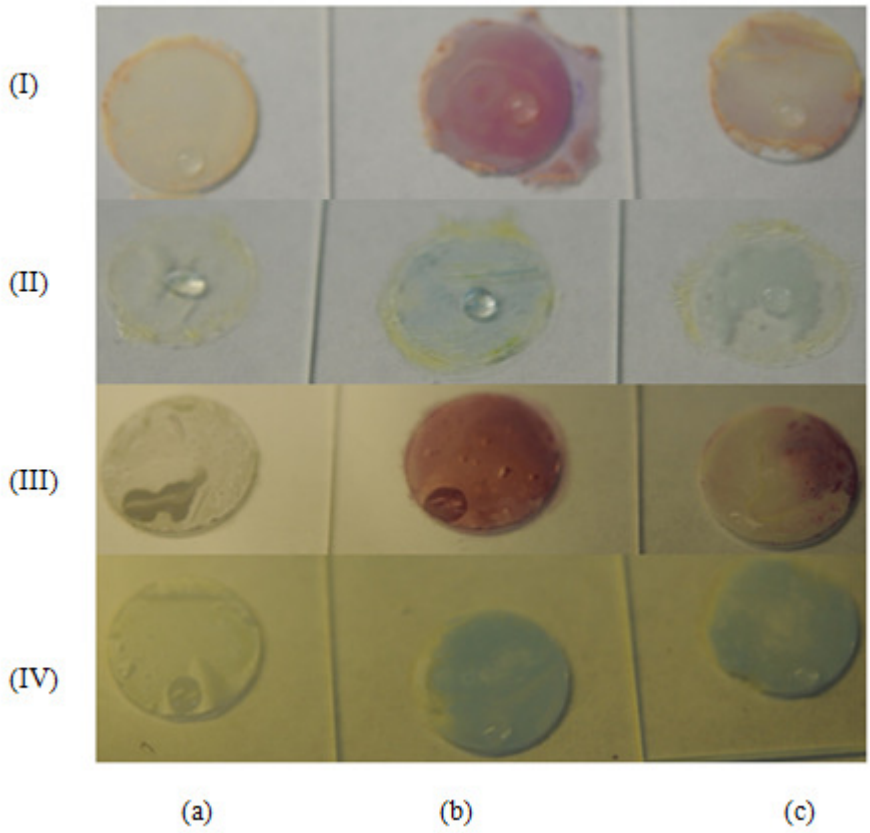

Figure 11: Photochromic experiments for solutions on polymer discs. Samples consisted of a 0.1 M solution of species 1 (Row I), a 0.1 M solution of species 3 (Row II), a 0.01 M solution of species 1 (Row III), and a 0.01 M solution of species 3 (Row IV). A-type samples were untreated (save room light), B-type samples were treated only with a UV lamp, and C-type samples were treated with the UV lamp and then with the visible laser. Differences may be observed in all rows. Also note that the contrast is almost more noticeable in the 0.01 M solutions as the untreated samples are whiter, and not super-saturated with spiropyran solutions.

Polymer disc type tests of photochromism were used again to determine the activity of the silane spiropyran synthesized in lab by Dr. Nammoonnoy. The test utilizing only 5 µL of the 1 wt% of the silane spiropyran in a solution of 3:2 DMF:EtOH did not seem to show changes, or they were difficult to detect. But at 10 µL the UV irradiated disc shows noticeable streaks of violet, and at 15 µL there are noticeable patches of violet after UV irradiation. These results may be viewed in Figure 12.

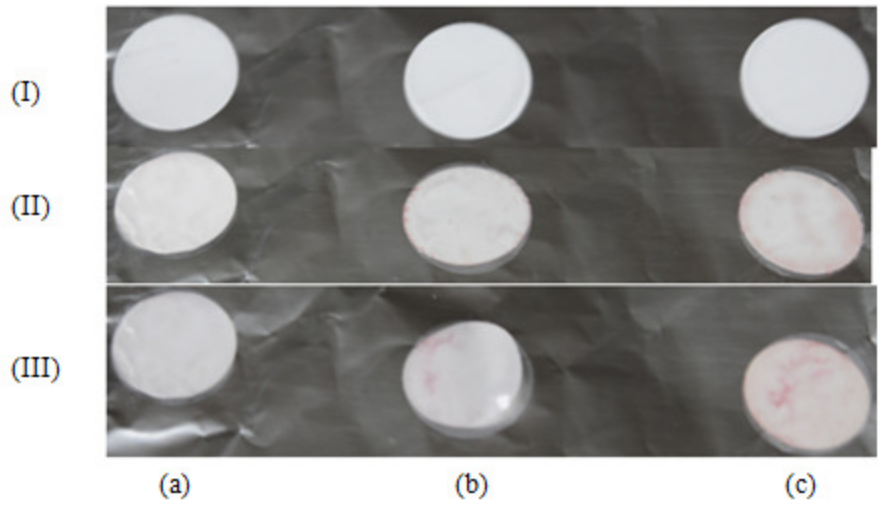

Figure 12: For the silane spiropyran experiment, three blank discs were placed on aluminum foil (row I). The discs had solution placed on them: 5 µL of the 1 wt% of the silane spiropyran in a solution of 3:2 DMF:EtOH (column a), 10 µL of solution (column b), and 15 µL of solution (column c). These were irradiated with visible light to ensure closed form (row II). They were then exposed to 15 minutes UV light (row III). There seems to be a noticeable increase in streaks for sample b, and whole patches for sample c, after UV irradiation.

A summary of all qualitative results can be seen in Table **1**. The summary of the quantitative results is that for those species that displayed a switch from MC to SP (#1 and #2), 45 seconds of laser light equaled or exceeded 5 minutes of room light in terms of the extent of the reverse transformation.

Table 1: A summary of the quantitative results for the polymer disc tests. The UV column refers to the transformation from SP to MC form. The room/laser column refers to a switch back to SP form in either room light or laser light.

Species	UV	Room/Laser Experiment
#1	Noticeable change	Noticeable change back
#2	Slight change	Slight change back
#3	Poor, no change	N/A
#4	Slight change	•Didn't readily switch back (neither room nor laser) •First sign that reversal could be a problem

1.4 Discussion

After the first solution experiment it was determined that species one had very good switching for the concentration that the solution was at. For species 2, the tint of the solution did not appear to change to a noticeable degree during any of these steps. The same was true of species 3; there was no noticeable change from its being a clear solution at this concentration.

It was thought that the solution of the concentrations might not be ideal for the switching of species 2 and 3. It was thought that species two might photochromically behave better at lower concentrations, where the saturation with color would not occur. It was thought that species 3 might behave better at higher concentrations, because while the stock solution was yellow the solution tested exhibited no change from being a colorless solution.

All solutions of species 1 tested exhibited noticeable changes in the UV/room light tests and in the laser tests. Species two showed slight changes for the UV/room light

tests (and as was predicted, showed no change at the higher concentration). The laser tests showed significant switching for species 2. Species 3 maintained poor performance in the UV/room light tests and in the laser tests. Species 4 showed slight changes in the UV/room light test and, interestingly, proved more difficult to switch back with the laser tests. Quantitatively, for those species that did switch in the UV/Laser test, switching occurred rapidly (45 seconds) when compared with an equal or lesser amount of switching in room light (5 minutes). Therefore, the theory of monochromic light of a certain wavelength affecting the equilibrium between forms seems to hold true.

It was decided that species 1 would be used for the polymer disc test because of its proven switching. Species three was chosen in the hope that the polymer disc tests (which more closely resemble the concentrations and amounts of solution that would be deposited in the electrospinning process) would prove more effective than the solution tests. Indeed, all polymer disc experiments proved effective for the species and concentrations used. This is a good sign for the types of room-temperature switching desired in photoswitching applications, and a good sign for the concentrations and deposition amounts desired in electrospun-deposited spiropyran.

Furthermore, it was useful to have the polymer disc procedure prepared for when it was desired to test the spiropyran species synthesized in-lab by Dr. Nammoonnoy. These tests showed noticeable switching for certain quantities of the solution.

1.5 Conclusion

The validity of room temperature photoswitching was studied and qualitatively proven to develop a better understanding of the spiropyran species that are desired to use

in direct-functionalization and electrospinning methods. It was shown through a systematic study of spiropyran solutions and deposits that room temperature photochromism is possible using ultraviolet and green-visible light. The green visible light was proven effective beyond the effects of room temperature and so the reversibility of this process was better understood.

It should be noted that the behavior of the photochromism depended on the species of spiropyran used and the concentrations at which they were studied. The nature of the transitions was also species dependent, with some species being harder to switch from MC form to SP form than others.

The polymer disc photochromic test that was developed, though qualitative, was still very useful in determining the validity of using lab-prepared spiropyran in the electrospinner. As research moves into direct functionalization of physically modified surfaces and electrospinning with spiropyran species, the important of having done tests to understand the photochromic behavior of several spiropyran species at room temperature and low concentrations will be apparent.

Chapter 2: Photoactuated Droplet Microfluidics

2.1 Introduction and Background

2.1.1 Traditional Microfluidics

The term "microfluidics" describes technologies that manipulate fluids in scales best described in micro liters per time period or lower. Typical microfluidic devices comprise channels on the order of tens to hundreds of microns in width. Microfluidic technology saw major development starting in the 1980s when applications such as ink jet printing and space-related technologies (*8*). Microfluidics sees large growth today in many biotechnological applications. It can be viewed that microfluidic technology is an inevitability stemming from several motivational forces. The development of analytical methods that required microscale samples, such as gas-phase chromatography, along with the development of photolithography and the success of microelectronic and microelectromechanical technologies led necessarily into the development of microfluidic systems (*9*). While early microfluidic systems did take advantage of photolithography in glass and silicon substrates, it was quickly realized that polymers (such as poly(dimethylsiloxane), i.e. PDMS) allowed for much easier fabrication (*9*). Polymers are relatively cheap, soft, and transparent. Research today continues to take advantage of a wide swath of substrates.

Microfluidics is an important development that has allowed for the ability to use small sample sizes and small amounts of reagents. This combined with the increased resolution and sensitivity afforded by microfluidics has allowed for procedures that are cheaper and take less time (*9*). Additionally, the nature of working with fluidic samples on the micro scale has revealed interesting properties involving the tendency of these

systems towards the laminar flow regime. Having a smaller quantity of reagents is safer when the reagents are dangerous, and means that the potential for automation, parallelization, and portability are all increased (*8*). The field of microfluidics has to deal with several challenges, including the reinvention of devices that can serve as pumps, valves, and mixers, the need to deal with volumes of materials on the micro scale, and the physical behavior changes in microfluidics (low velocity, large surface area to volume ratio). (*8*)

The list of applications for microfluidics is huge. A small sample of applications of microfluidics include molecular separation techniques, Control systems and heat management, energy generation, display technology, protein crystallization, proteomics, micropumps, clinical applications, forensic applications, sample pretreatment, molecular diagnostics, separation techniques, DNA separation, polymer electrophoresis (*10*).

2.1.2 Droplet/Digital Microfluidics

Droplet microfluidics, also called digital microfluidics, is a term that can be used to describe two types of systems. One type of droplet microfluidics utilizes mechanisms that are much more similar to traditional microfluidics, in which droplets are carried by a carrier flow in a traditional microfluidics set up. The other type of microfluidics involves entirely novel mechanisms for transporting droplets. One such technique is electrowetting, in which a charge is used to move droplets.

Droplet microfluidics requires even smaller working volumes than traditional microfluidics. It therefore has all of the benefits of microfluidics to an even greater extent: increased speed, decreased danger in working with hazardous reactants, etc.

Droplet microfluidics makes more sense when discrete samples with specific volumes are required, in comparison to a flow system (*11*). Additionally, it solves some adherence/adhesion problems that exist in microflow systems (*8*). There are disadvantages to droplet microfluidics as well, such as the problem of droplet evaporation (*11*).

One type of droplet microfluidics recently developed as an Oregon State University Honors Thesis was Beth Dunfield's *Mechanically Actuated Droplet Microfluidics*, which explored the use of a stylus to mechanically force droplet motion on hydrophobic surfaces. This thesis demonstrated MADM as a viable method of droplet microfluidics with promising results in a PCR application (*12*).

2.1.3 Photoactuated Droplet Microfluidics

As was covered in the introduction to this paper, it is proposed to prove a viable method of droplet microfluidics using the photoactuation of spiropyran molecules. It must be noted that photoswitchable wettability and photoswitching for mobility applications do already exist, to some degree, in the literature.

The use of a monolayer of azobenzene on a silica surface to move a droplet of liquid via a mechanism of asymmetric photoirradiation was described previously, (*13*). This group was successful in moving olive oil droplets on the azobenzene surface, as well as moving NPC-02, which is described as a binary mixture of 4-pro-pyl-49-ethoxy- and 4-propyl-49-butoxyphenyl-cyclohexanes, in an azobenzene-functionalized glass tube (*13*). Similarly, photoswitchable mobility of glycerol drops on an azobenzene/liquid

crystal emulsion has also been proven, (*14*). Photoactuated movement of oleic acid droplets in an azobenzene solution has also been shown, (*15*).

It is hoped that the research of this paper can show photoactuation of spiropyrans as a viable method for a photoactuated droplet microfluidics system. The significance of a new type of droplet microfluidics would be wide-reaching. A photoactuated system would allow for quick, remote, and accurate control of a droplet. For instance, due to the nature of a photoactuated system having light as a driving force, the risk of contamination in biological microfluidic applications (such as PCR) is reduced considerably.

2.2 Materials and Methods

2.2.1 Physically Modified Surface – Pillars

Several physical systems were proposed to demonstrate photoactuated mobility in a functionalized surface. One such system was the development of a physically modified surface of "posts" resembling an undulating sinusoidal-wave with amplitudes of 25, 50, and 75 microns. The primary idea behind posts was maximization of the surface area that contacts the droplet.

2.2.1.1 Laser Cutting

In order to make the planned posted system, a system of criss-cross lines was created in SolidWorks, see Figure 13. When the laser cuts into the polymer, it does so in the shape of a Gaussian curve. It was hoped that the criss-cross system would lead to undulating, sinusoidal curves in three dimensions, thus forming a shape like egg crate

foam. The dimensions on the SolidWorks file were a 1cm by 1.5 cm grid consisting of diagonal parallel lines with 100 micron spacing between each diagonal line.

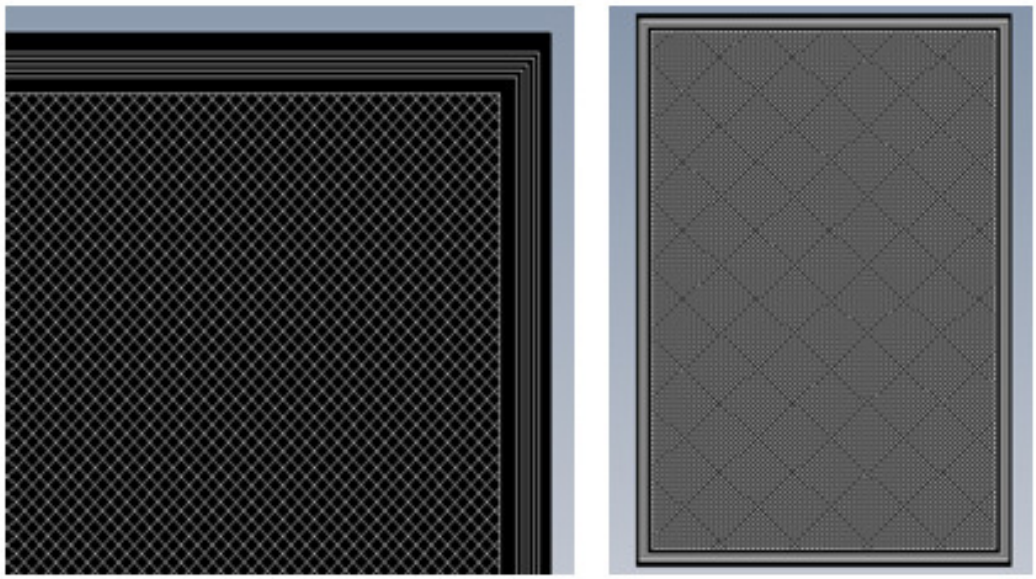

Figure 13: The design for the grid system, which would lead into the tool path for the posts.

This design was transferred to a G-code tool path using SmartCAM Advanced Fabrication v15. This was uploaded to the laser machining tool, an ESI 5330 UV Laser Drill. The ESI 5330 was run with a z-offset of 2.000mm, a velocity of 200.00 mm/sec, a rep rate of 30.000 kHz, and a power set at 5.6 Watts. The tool was used to cut six grids into PEI, two grids at 2 repetitions of the laser, two grids at 4 repetitions of the laser, and two grids at 6 repetitions of the laser. See Figure 14.

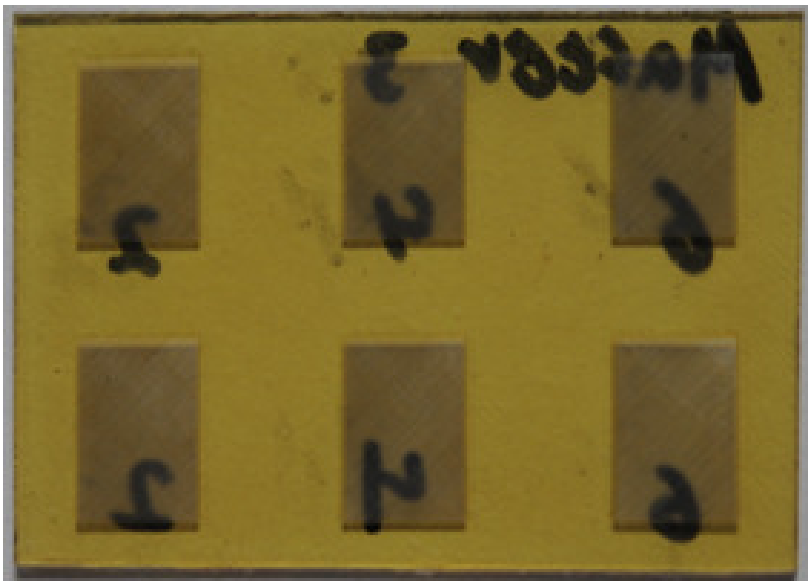

Figure 14: An example PEI master. The left-hand column contains grids that were made from 2 repetitions of the laser, the middle column used 4 repetitions, and the right-hand column used 6 repetitions.

2.2.1.2 Nanoimprinting

A Jenoptik nanoimprinter was used for hot embossing. This step was used to transfer the features from PEI to PMMA, which is the polymer necessary for spiropyran functionalization. The nanoimprinter serves to bring the PMMA to a temperature just above its glass transition temperature, and then apply so much pressure that the PMMA flows into the PEI master like gelatin in a mold. As the feature is reversible (it is alright if the peaks in the post system become valleys), a single pass was used.

The instrument utilized contact temperatures of 168.0 °C for the upper plate and 153.0 °C for the lower plate. Substrates were held at 144.0 °C for the PEI (on top), and 140.0 °C for the PMMA substrate (bottom). The force applied was 50,000 N for a period of 300 seconds. Given that the average area of the chips were 0.0029 m^2, the operating

pressure works out to about 17.1 MPa. An example of a PMMA chip made from this process can be seen in Figure 15.

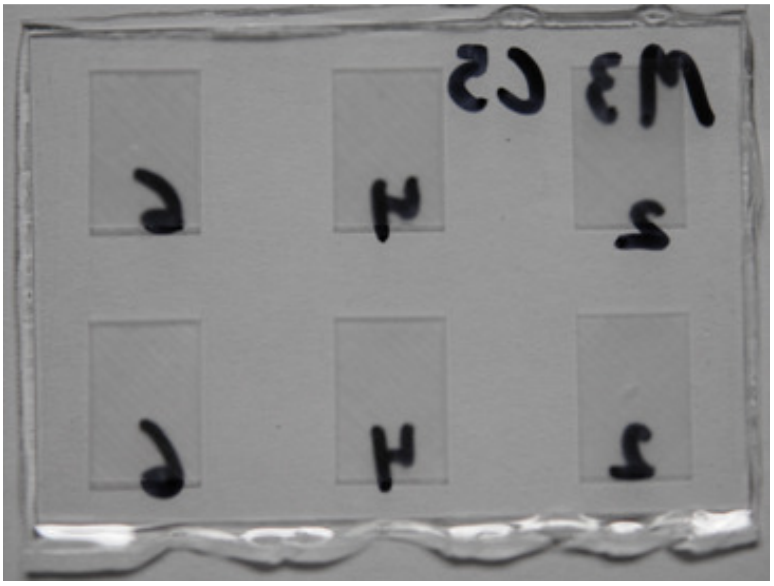

Figure 15: A PMMA chip embossed from the PEI master described in Figure 14.

The chips then had optical profilometry and microscope camera images captured in order to establish the physical metrology of the features. A ZeScope Optical Profiler was used for metrology

2.2.2 Direct Functionalization with Spiropyrans

The nature of the PMMA posts' wettability was rudimentarily established by taking pictures using a Dinolite Pro Digital Microscope in order to establish the nature of the material. Methacrylic acid monomer was distilled to remove inhibitors. This was in turn mixed with 3 wt% 2,2-dimethoxy-2-phenyl acetophenone (DMPA) – a photoinitiator. The solution was placed on the posts and allowed to absorb for five minutes, before it was spin-coated off at 500 rpm for 15 sec and then 1000 rpm for 30

sec. The chip was then allowed to photopolymerize under UV light (254 nm) at a distance of 10 cm for at least 24 hours. The result of this step can be seen in Figure **17**. The chip was then washed for an hour with DI water and dried with N_2 gas. The contact angle was checked to see if there was a change, indicating that the PMMA surface was now in carboxylic form.

The chip was then immersed in an 1-ethyl-3(3-dimethylaminopropyl) carbodiimide (EDC) solution (2.5 mg/ml DI water) for ten minutes, and then had 1-8, Diaminooctane purum added at 5.5 mg/mL, at which point the system was stirred for at least 24 hours. This step can be seen in Figure **17**. The chip was then washed for a half hour with 1:1 EtOH:DI, then rinsed with DI water and dried in N_2 gas. The chip was immersed/stirred for at least 36 hours in a solution of 3:1 DI/EtOH, 2.5 mg/ml EDC, and 2.5 mg/mL spiropyran (JN-1-242, synthesized by Dr. Jintana Nammoonnoy). This spiropyran is 1'-(3'-carboxypropyl)-3',3'-dimethylspiro[2H,1]benzopyran-2,2'-indoline, and can be seen in Figure 16. The chips were then washed with 1:1 EtOH/DI, washed with DI, then EtOH, then dried with N_2 gas. This final step can be seen in Figure 17. At this point photochromism and contact angle could be checked to ensure functionalization had occurred.

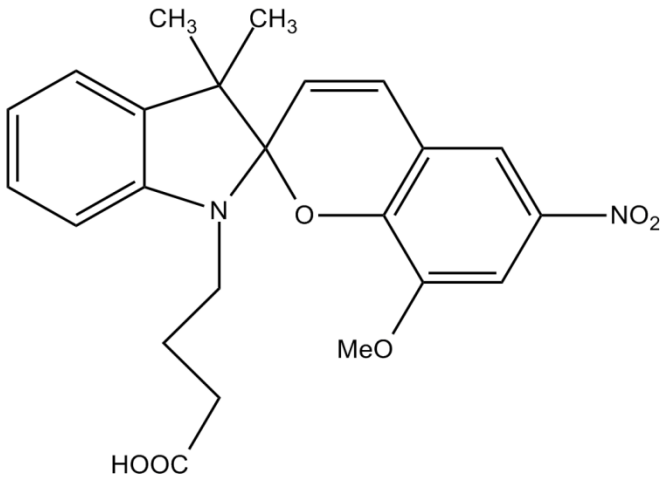

Figure 16: Spiropyran species JN-1-242, 1'-(3'-carboxypropyl)-3',3'-dimethylspiro[2H,1]benzopyran-2,2'-indoline.

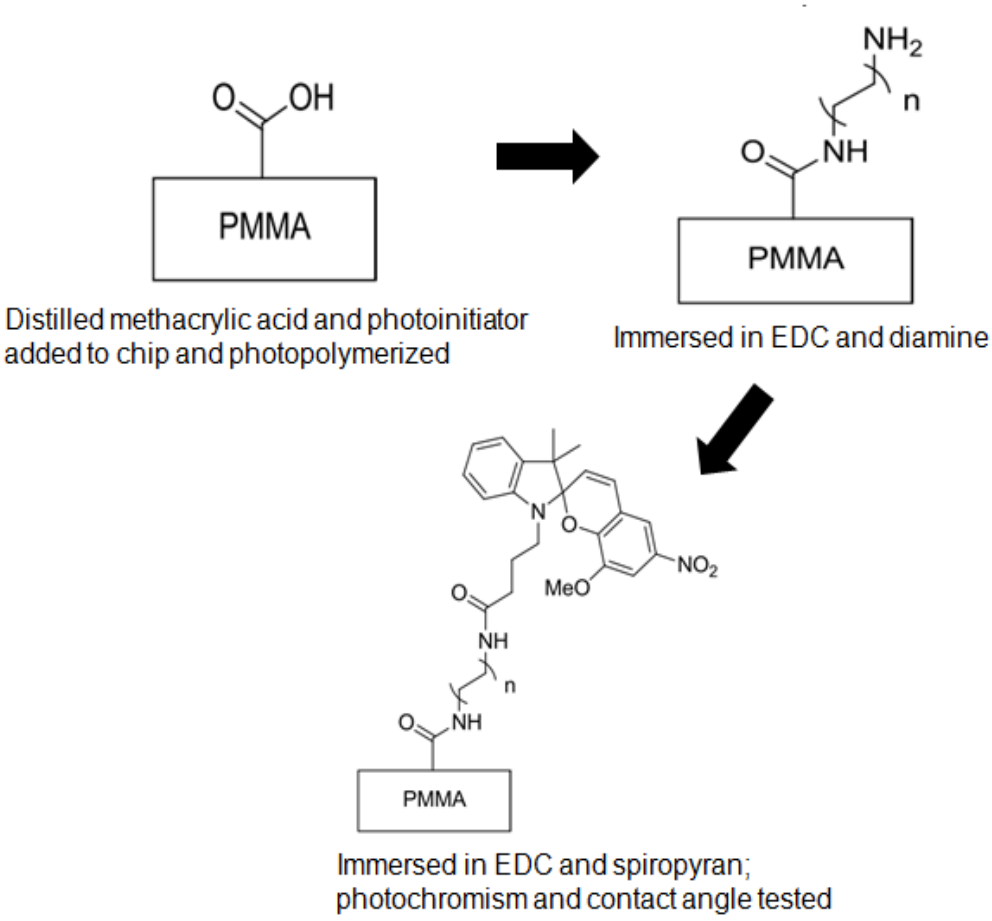

Figure 17: Brief summary of the functionalization procedure in terms of the organic reactions at the substrate surface. Based on images/description by Dr. Nammoonnoy (*16*).

2.3 Results

2.3.1 Physically Modified Surface – Pillars

As mentioned previously, a ZeScope Optical Profiler was used for metrology. The actual pillars were successful – they came out to resemble the desired morphology (an egg-crate foam style system of posts). The typical amplitude was 35 microns and the typical pitch was 100 microns. All grids, at 2, 4, or 6 passes had these dimensions. Though the grids with 6 passes seemed to be deeper on average, and the whole 6 pass system stuck out of the PMMA further than the 2 pass system. An example of profilometry images can be seen in Figure 18.

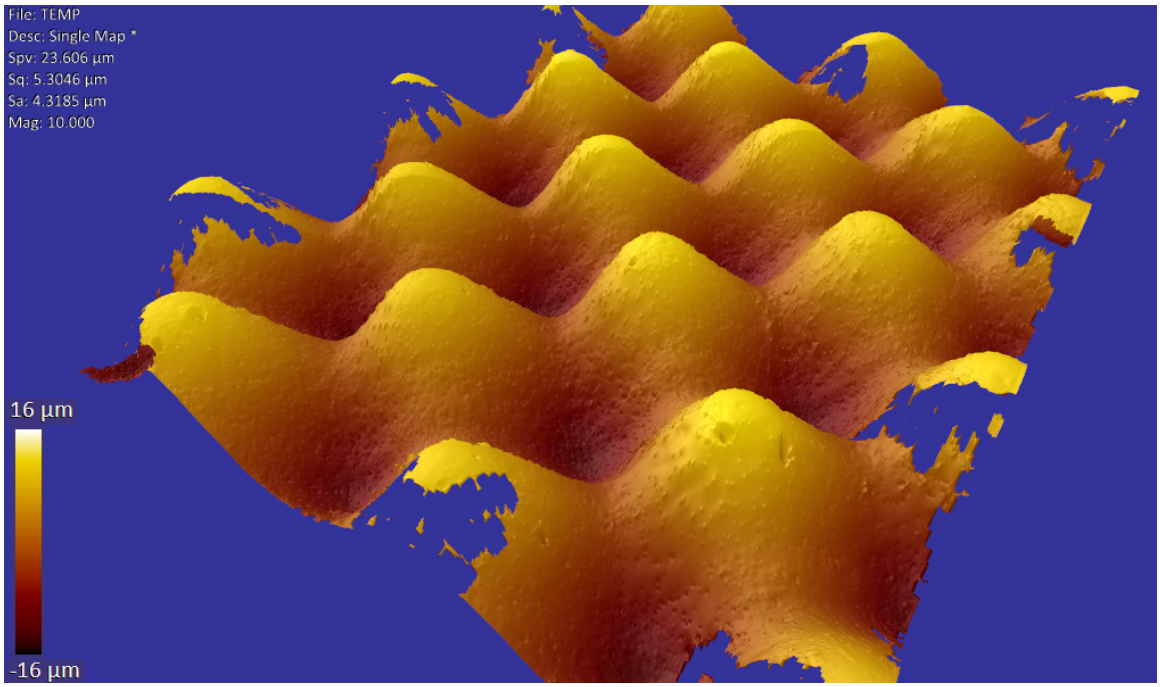

Figure 18: Profilometry of the pillars revealed dimensions of 35 microns in amplitude and 100 microns for a pitch. Note that this applied for all samples, at 2, 4, or 6 passes.

2.3.2 Direct Functionalization with Spiropyrans

Functionalization of the chips took several trials of the procedure. Finally, when purer PMMA from GoodFellow was used in hopes of eliminating the effects of additives, the chips functionalized. The photochromic test that proved this can be seen in Figure 19. The posts seemed to be maintained in terms of their structure, as can be seen in Figure 20.

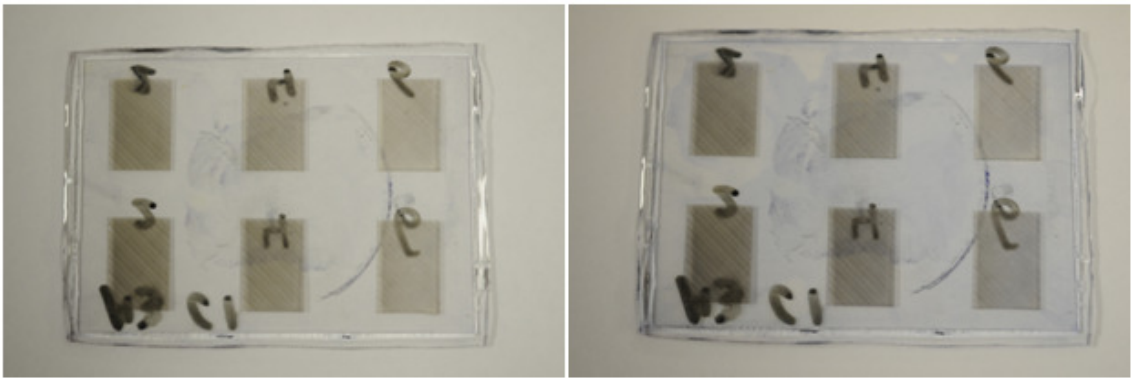

Figure 19: The chip before exposure to UV light can be seen on the left. The chip after UV lamp exposure for 15 minutes can be seen on the right. Notice the appearance of a blue tint after UV exposure.

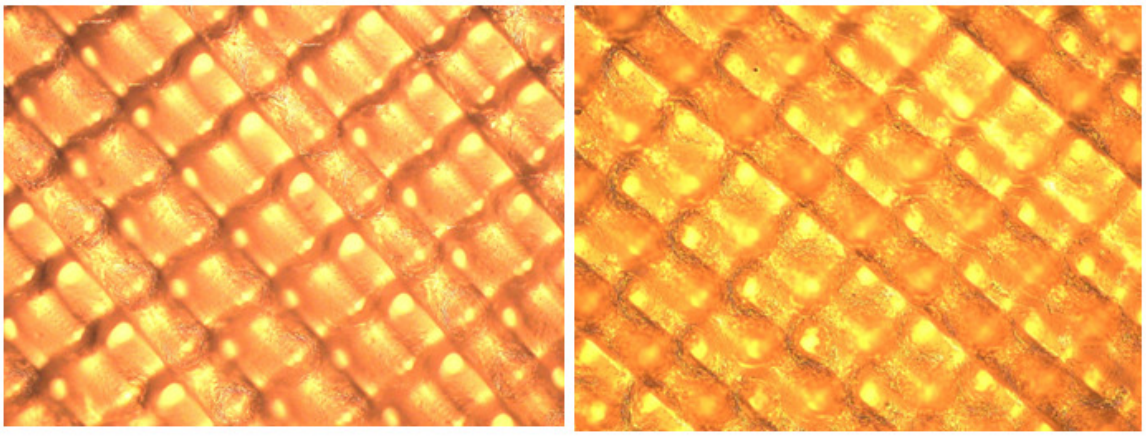

Figure 20: The posted system before the functionalization process (left), and after (right). Notice that the structure seems to remain intact.

Contact angle experiments were performed on two of the functionalized chips. The results show a change in wettability on the posted systems after exposure to UV irradiation. See Figure 21 and Figure 22. The data leading to these plots may be found in Appendix 1.

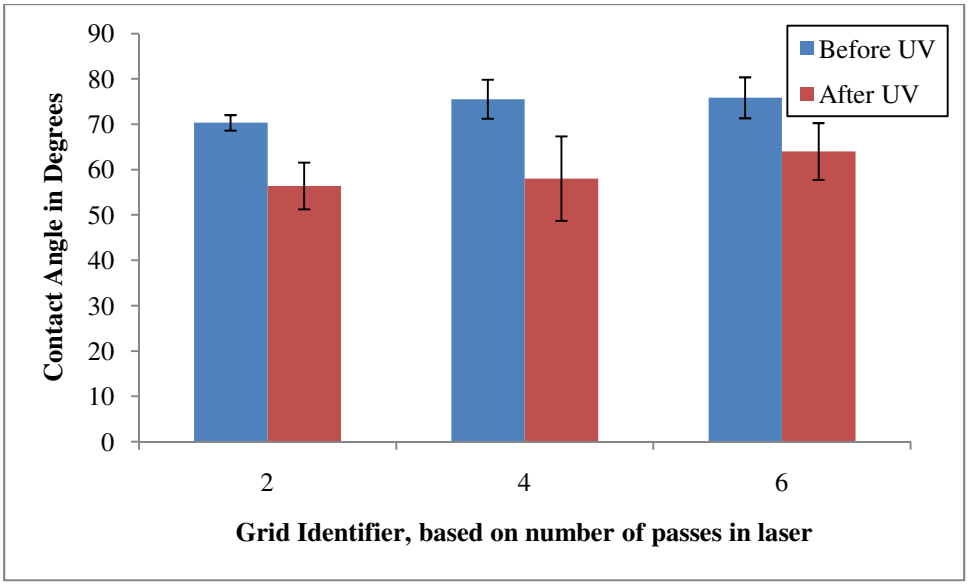

Figure 21: Plot of grid-type versus contact angle for the first chip before and after exposure to UV irradiation. Notice that UV irradiation seems to lower the contact angle. Error bars based on four repetitions of data samples at 90% confidence.

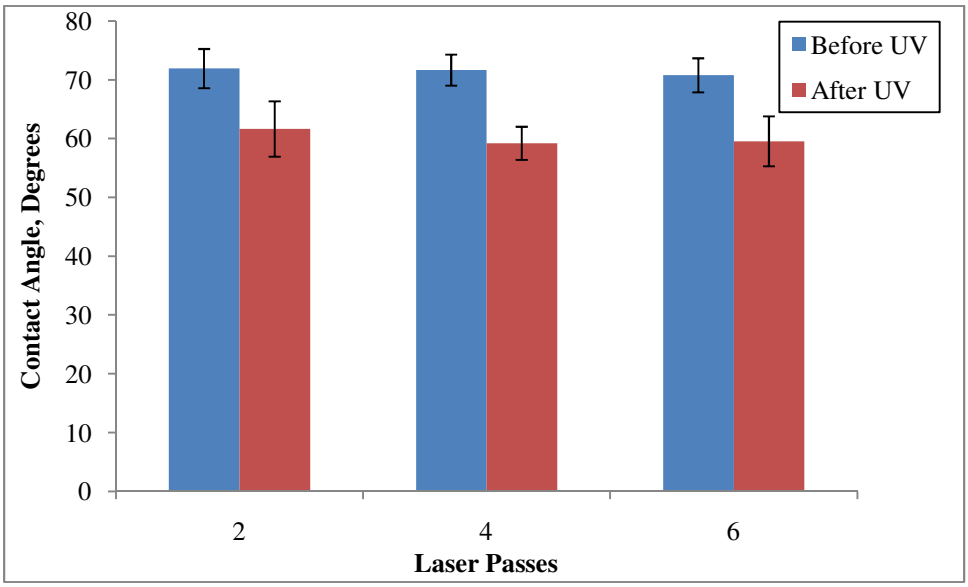

Figure 22: Plot of grid-type versus contact angle for the second chip before and after exposure to UV irradiation. Notice that UV irradiation seems to lower the contact angle. Error bars based on eight repetitions of data samples at 90% confidence.

An analysis of variance, the full extent of which may be viewed in Appendix 2, reveals a noticeable change in wettability in both chips before and after treatment with UV irradiation. For the first chip, with four repetitions of data per grid, the p-value was 1.17×10^{-6}, which is small and implies that there is a very small chance that the treatment had no effect. The treatment of the second chip at eight repetitions of data showed even better results, with a very small p-value of 4.71×10^{-9}.

2.4 Discussion

Physically modified PMMA chips were manufactured via laser drilling and hot embossing. A series of undulating posts resembling egg crate foam were successfully created, and profilometry revealed them to be of the intended metrology.

The posts were then chemically modified to incorporate spiropyran molecules on their surface. Chips were successfully modified as revealed by photochromism and wettability tests. Furthermore, the chips were photoswitchable in terms of their wettability.

2.5 Conclusion

In light of the ongoing development of microfluidics, and specifically droplet microfluidics, it was sought to come up with a novel method of realizing photoactuated droplet microfluidics. Direct functionalization of a physically modified surface with spiropyran molecules is one such method. In the process of reaching this goal, physically modified chips were successfully manufactured and functionalized.

What remains to be seen is if the actual act of photoactuated mobility is possible. It seems that since UV irradiation has been shown to create a change in contact angle, then asymmetric irradiation on the posted surface should create a wettability gradient. Whether or not this could serve as a realistic driving force for a droplet would depend on the nature of the droplet in terms of surface tension. Further testing remains, but the research done thus far is a step in the right direction towards a photoactuated system.

Chapter 3: Electrospinning

3.1 Introduction and Background

There is another possible method for photoswitchable wettability. After the publication of Dr. Jintana Nammoonnoy's dissertation, *Photoactivable Microfluidic Device for Heavy Metal Ion Extraction*, her and Dr. Myra Koesdjojo brought to Dr. Remcho's research group the idea of using the process of electrospinning to create spiropyran functionalized polymeric nanofibers. It was proposed that nanofibers functionalized with spiropyran would present similar photoswitchable properties, i.e. photochromism, wettability change, and the possibility for filtration application similar to Dr. Nammoonnoy's previous work, but would present a morphology with a more desirable active surface area.

In the process of electrospinning, a high-voltage electrical potential is applied between the needle of a syringe and a collector (typically a plate). The syringe houses a polymer solution, or melt, and is attached to a syringe pump. As the pump is activated and the polymeric solution flows out of the needle, the electrostatic field forces the droplet to take the form known as a Taylor Cone. If the electrostatic force is high enough, a charged jet of solution will be emitted from the Taylor Cone. As the jet flies from the needle to the collector, the organic solvent is evaporated and the polymer splays, where splaying is defined as the separation of the polymer due to mutual repulsion of like charges, (*17*). Research revealed that while the electrospinning set-ups are generally similar, there are modifications that can be made to the base design and there are a few key parameters that can be optimized.

Electric Field Strength

Each polymer/solvent system has an optimum range for the strength of the electric field applied to it, proportional to net voltage divided by net point-to-plate distance. The maintenance of the field within an optimum range is necessary to the electrospinning process, and this must be considered as the applied voltage and point-plate distance are optimized.

Applied Voltage

An increase in the applied voltage will cause a decrease in the diameter of the spun nanofibers, to a point, and after a minimum is encountered the fibers will increase in diameter (*18*). It was later found during the optimization of our electrospinner that the increase in fiber size after a minimum described in (*18*) may refer to the fact that if the electric field strength is too high the fibers polymerizes to quickly and form "webs" of polymer in the space between the needle and plate.

Point-Plate Distance

An increase in the distance between the needle and the plate results in a decrease in the diameter of the nanofibers, and also reduces the chance of beading (*18*).

Flow rate

The creation and maintenance of the Taylor cone is dependent on flow rate – the flow rate must be balanced so that the flow out of the needle replaces the mass of polymer solution being spun at a given point in time, and is neither higher nor lower than

this amount. If the flow is too low then the Taylor cone doesn't form. Previous research showed that as the flow increases the nanofibers diameter increases, as well as the pore size and amount of defects (*18*).

Solution properties

The concentration of the polymeric solution affects viscosity. The concentration is limited to a region that depends on the solvent and solutes, and an increased viscosity leads to an increased diameter (*18*). In addition, the properties of the organic solvent used (volatility and conductivity) have an impact on the morphology. Increasing the conductivity leads to a decreased fiber diameter, and increasing the volatility leads to an increasing in microtexturization (which increases the available surface area) (*18*).

From these relationships it became apparent that if we desired small fibers and an increased surface area, we would need to make the voltage as high as possible, the flow rate as low as possible while still maintaining a Taylor cone, the distance as high as possible while still maintaining a strong enough electric field, the concentration as low as possible, and the solvent's conductivity and volatility as high as possible. A detailed literature review was conducted to get a feel for numerical values reported by other groups who felt that they had optimized an electrospinning system.

One previous system did not use the traditional point-plate system, but instead the target consisted of a sharp, charged needle placed inside of a rotating cylinder. The needle was charged via a wire threaded through the syringe. This group also used lower distances and voltages, believing that a smaller distance would allow for more controlled

spinning. The voltage used was 4.5 kV, the point-point distance was 1 to 3 cm, and the solutions were 15, 20, and 25 wt% PS and PMMA in tetrehydrofuran and chloroform (*17*). This worked, but produced relatively high-diameter fibers when compared with previous literature (1-10 microns).

Another group utilized the traditional point-plate setup. This group used voltages of 5.5-15.0 kV, solutions of 4-10 wt% PEO in HPLC grade water, a 23g needle, a 16.5 cm point-plate distance, and utilized various targets, such as an aluminum screen (*19*). The system was set up vertically, with the needle aiming down and the target below it. This group found that increasing viscosities increased the diameter of the fibers and made the system more difficult to control, with reduced deposit rates (*19*). For their parameters, fiber diameters were on the sub-micron order (0.15-0.4 microns) (*19*).

Electrospinning with spiropyran for the creation of photochromic nanofibers has been done before, with the result that the photochromic behavior was preserved (*20*). In this previous research 10, 15, and 20 wt% polyvinylidene fluoride solutions in 3:2 DMAc: Acetone were tested with 1wt% of a spiropyran species. A point-plate assembly with an aluminum foil plate, 7kV potential, 0.9 mL/hr flow rate, and 25cm point-plate distance was used in the electrospinning setup (*20*). It was desired to emulate this research in terms of the maintenance of photochromism in electrospun fibers, while customizing the parameters on the electrospinning setup to create fibers of a desired morphology. The desired morphology was maximal surface area and minimal fiber diameter.

3.2 Materials and Methods

3.2.1 Construction of the Electrospinner

An electrospinner was constructed, modeled after commonalities in the design of electrospinners taken from our literature reviews. The electrospinner was constructed to safety specifications discovered in literature, as well as safety advice from the OSU Chemistry Department's electrician Mark Warner.

A large chamber of dimensions 2ft by 2 ft by 4 ft was constructed from sheets of PC for the walls and posts of PP for the posts. The primary concern when constructing this box was to ensure that no metal pieces were exposed to the inside of the box. For this reason, the box was built in such a way that screws were screwed through the walls into the posts and securely fastened. In this way the chamber was secure, but all metal remained unexposed, see Figure 23.

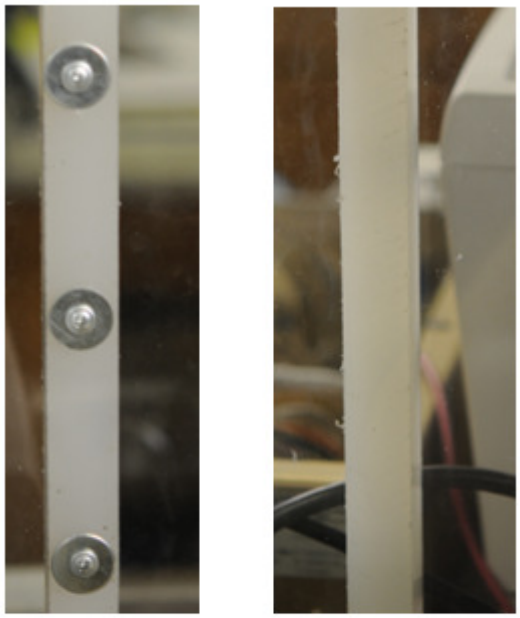

Figure 23: Image of the construction of the electrospinner. (a) The outside of the electrospinner, notice the screws go into the sheet and column. (b) The inside of the electrospinner, notice that no screws are exposed to the inside.

Features on the chamber included a sliding door in the front of the chamber, holes big enough to fit electrical cords for AC power cords and also for the DC power supplies' leads. Also included was a large hole for ventilation (this hole directly led into the piping and fan system.

The secondary power supply was outside the chamber along the edge of the chamber closest to the fume hood. A hole was drilled on this side to allow for the positive power lead to thread through. On the inside of the power supply the target mounting block was placed immediately next to the secondary power supply. The needle mounting block for the needle was placed 18 cm away from the target mounting block. The syringe pump was placed far away from the needle mounting block, and a hole was drilled into the chamber to allow for the syringe pump's electrical supply cord. The primary power

supply was placed behind the chamber such that its negative lead could reach the needle mounting block. Finally, a large hole was drilled on the side of the chamber closest to the fume hood, just above the place where electrospun fibers would hit the target. In this hole was placed a large PVC fitting which forms the inlet to aluminum piping which connect to a powered fan, and then leads with more pipe into the fume hood.

The main power supply is a Spellman CZE1000R, [0-30 kV, 0-300 ua]. This provides the system with the positive DC voltage lead to the syringe needle, which can be set between 0 to 30 kV. The secondary power supply is a Bertan Associates Inc. Series 230, [0-3kV]. This provides a negative charge to the target substrate, and is always set at 3 kV. The syringe pump is a Harvard Apparatus: PHD 2000 Infuse/Withdraw syringe pump.

Syringes are typically BD 3mL syringes with a Luer-Lok™ Tip. The needles typically used in the system are 27g needles. Typical target substrates are N-type silicon wafers, polished on both sides, with a 40-64 ohm-cm resistivity, (1-1-1) ±1° orientation, 75.6-76.8 mm diameter, and 228 ± 15μm thickness from University Wafer. Other substrates used include glass (with a conductive, typically aluminum, backing), filter paper or membranes (with conductive backing). The PMMA that is the typical polymer solute is Spectrum P2845, CAS = 9011-14-7.

An image of the electrospinner may be found in Appendix 3.

3.2.2 Electrospinning Procedure

The following is an example of the standard procedure for electrospinning on a substrate. The parameters described will be for optimal fibers (small with no beading)

with aryl silane spiropyran on a silicon wafer substrate. For a more general procedure, the Remcho Lab group's Electrospinning SOP (Frederick and Fuchs 2010) may be found as Appendix 3. The methodology that was undertaken to derive the following procedure, i.e. the optimization of the electrospinner, is described in section 3.2.3.

Before reading through the following procedure, keep the following safety related material in mind. Gloves and safety glasses were always worn when dealing with the solution or the chamber. The chamber was always allowed to vent immediately following electrospinning to allow the concentration of organic solvents and nanofibers in the chamber to be significantly reduced. The chamber was never opened while the power supplies are on. After an electrospinning run neither the needle nor substrate were touched until they had been discharged.

The polymeric solution was prepared. This required measuring out an appropriate quantity of organic solvent, 3:2 DMF: EtOH. PMMA was added to the solution at 20 wt%. The solution required a significant amount of time to dissolve, and it was important to dissolve the polymer in the organic solvent well ahead of time; devices such as vortexes and vial rotisseries aided in the dissolution. When polymer was thoroughly mixed, the functional spiropyran molecule was added in the appropriate amount at 1 wt%. The solution was immediately wrapped in aluminum foil to prevent photo bleaching and was again thoroughly mixed.

The polymeric solution was then drawn into a 3 mL syringe. An appropriate Upchurch fitting was screwed into the syringe head such that it could be connected to Teflon tubing (a safety assessment by our resident electrician indicated that it is important to have a length of Teflon tubing between the syringe pump and needle to

prevent damage to the syringe pump by the high-voltage lead). The other end of the Teflon tubing was threaded through another appropriate Upchurch fitting such that it could be connected to a 27g needle. The syringe was placed in the syringe pump and the needle was mounted on the mounting block, fastened securely with duct tape. The positive lead was attached to the needle.

The desired substrate, typically a silicon wafer, was placed in a slot on the substrate mount 18 cm away from the tip of the needle. The negative lead was attached to the back of the silicon wafer with electrical tape. The syringe pump was plugged in and had its settings set for a diameter of 8.66 mm for a 3 mL syringe and a flow rate of 0.4 mL/hr. The pump was set to "infuse." The end of the exhaust duct was placed into the fume hood, and the power supplies were plugged in. Without turning them on, the negative power supply was set to its maximum setting, 3 kV, and the positive power supply was set to 8 kV. The syringe pump was used to push the solution into the tip of the needle such that the solution just started to come out of the needle. This was done slowly to avoid building up pressure in the needle.

When both operators were ready, the needle was wiped clean and the syringe pump was started. The door to the electrospinner was shut and both power supplies turned on as expediently as possible to avoid the solution drying at the needle's tip. The system was observed to ensure that the spinning process began. The needle was observed to ensure the solution was leaving and forming a Taylor cone, and the substrate was observed for an accumulation of fibers. If the needle appeared clogged or the fibers polymerized too quickly and flew around the chamber, then the process was aborted. The system was run either until the passage of a desired time during optimization experience,

or the observation of a desired quantity of coating. When the spinning was determined to be sufficient, both power supplies were shut off. The system was kept closed for several minutes to ensure proper ventilation. As soon as the chamber door was opened, a discharging rod consisting of a copper wire threaded through a semi-hollow glass tube was utilized to remove any remaining charge from the needle and substrate. The syringe pump was turned off. The mounted substrate was removed, cleaned (on the back), and placed immediately into a Petri dish. The Petri dish was wrapped in aluminum foil to prevent the possibility of photo bleaching. At this point the electrospinner was either used again on a new substrate, or was cleaned up.

3.3 Results

The optimization of the electrospinner was a very detailed process requiring us to spin dozens of samples and examine the morphology via hundreds of images. What follows then is a summary of the results, where the results are groups by major changes to the electrospinning process that had a significant impact on the morphology. The easiest way to convey electrospinning morphology results is through images, so some representative images have been chosen for each category of results.

Results for Research Phase I: Initial parameters

For 5 wt% PMMA in chloroform with other parameter ranges of 15-20 kV potential, 25cm point-plate distance, a 25 g needle, and 0.5-0.75 ml/hr flow rates, electrospraying (and not spinning) was observed. Examples of this may be seen in Figure 24.

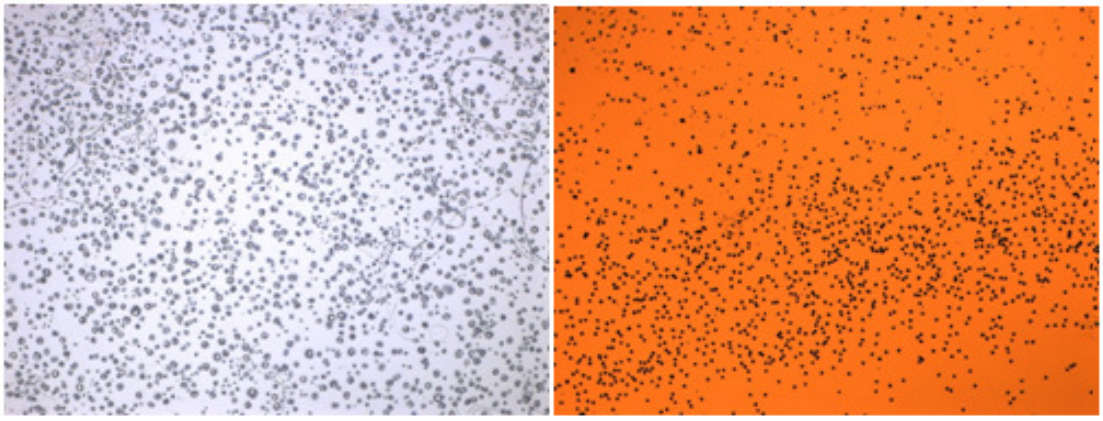

(a) (b)

Figure 24: Microscope images for electrospun samples with parameters of (a)0.5ml/hr flow, 5 wt% PMMA in chloroform solution, 20kv potential, and 25cm point-plate distance (b)0.75ml/hr flow, 5 wt% PMMA in chloroform solution, 18kv potential, 25 cm point-plate distance

Results for Research Phase II: Increased concentration, decreased flow rates

For 15 wt% PMMA in chloroform with parameter ranges of 15-20 kV potentials, 10-17cm point-plate distances, a 25 g needle, and 0.5 ml/hr flow rates, fibers were obtained. Parameters that reached higher voltage ranges resulted in a phenomenon where the solution would polymerize too quickly in the air, thus creating a sort of cobweb effect by the time it reached the actual substrate. Significant beading was observed in the spun fibers. The morphology can be seen in Figure 25.

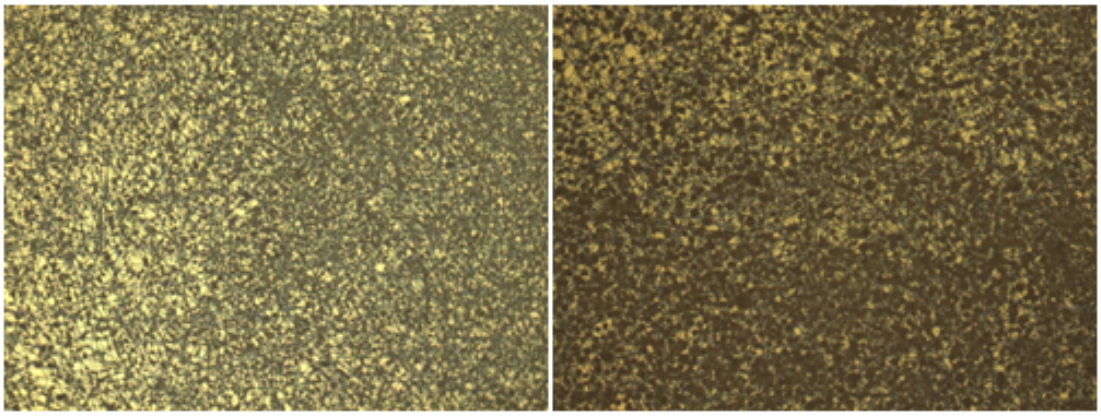

(a) (b)

Figure 25: Microscope images for electrospun samples with parameters of (a)0.5ml/hr flow, 15wt% PMMA in chloroform solution, 15kv potential, 17 cm point-plate distance (b)0.5ml/hr flow, 15wt% PMMA in chloroform solution, 20kv potential, 17cm point-plate distance

Results for Research Phase III: Spiropyran added

For 15 wt% PMMA and 1 wt% of various spiropyran species in chloroform with parameter ranges of 10-17 kV potentials, 10 cm point-plate distances, a 25 g needle, and 0.4 - 0.5 ml/hr flow rates, fibers were obtained. Significant beading was again observed in the spun fibers. The morphology can be seen in Figure 26. SEM images were taken at this time and confirmed the presence of fibers, but also beading, an example of this may be seen in Figure 27.

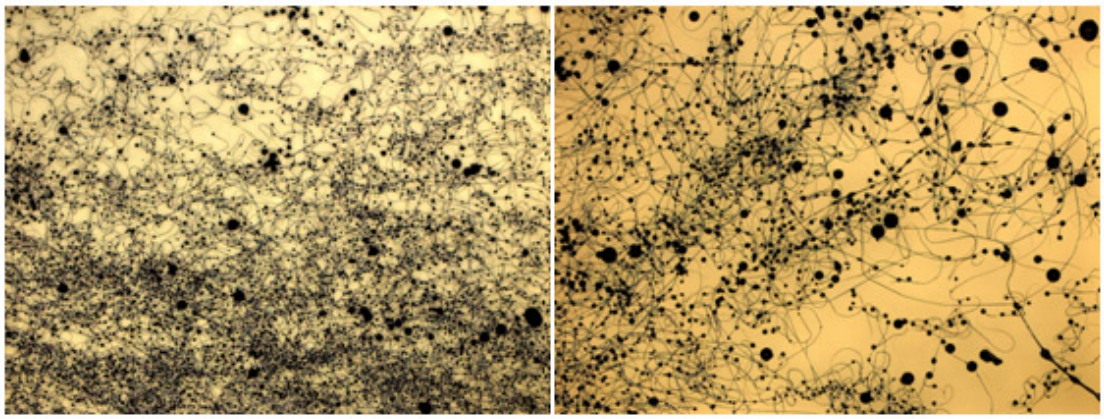

(a) (b)

Figure 26: Microscope images for electrospun samples with parameters of (a) 15 wt% PMMA; 1 wt% Spiro 2 in chloroform, 0.5 ml/hr flow, 10 cm distance, 12kv (b) 15;1 wt% PMMA;spiro3 in chloroform, 0.4ml/hr flow, 12kv,15cm

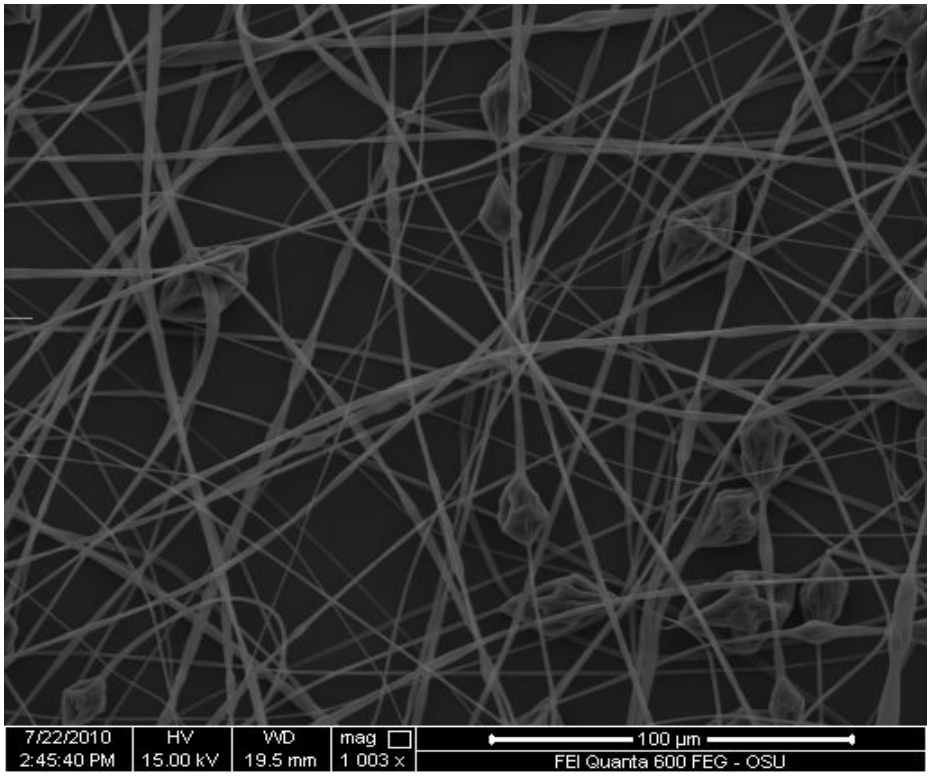

Figure 27: SEM image for a sample based on electrospun parameters of: 15 wt% PMMA, 1 wt% Spiro 3 in chloroform, a 23g needle, a 10cm distance, an 11 kV potential, and a 0.4 ml/hr flow rate

Results for Research Phase IV: Switch to DMF as a solvent

For 20 wt% PMMA and 1 wt% of various spiropyran species in DMF with parameter ranges of 10-15 kV potentials, 15-18 cm point-plate distances, a 27 g needle, and 0.4 ml/hr flow rates, fibers were obtained. Significant beading was again observed in the spun fibers. The morphology can be seen in Figure 28. SEM images were taken at this time and confirmed the presence of fibers, but also the continued existence of beading, an example of this may be seen in Figure 29.

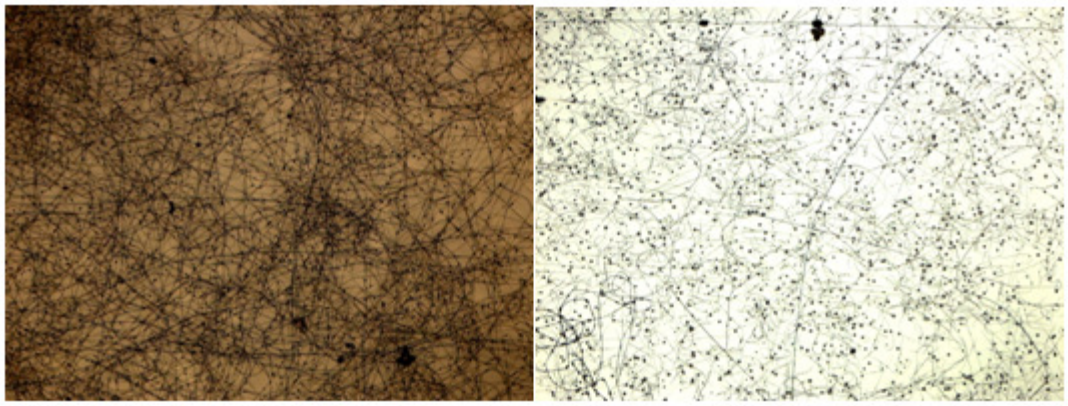

Figure 28: Microscope images for electrospun samples with parameters of (a) 20 wt% PMMA; 1 wt% Spiro 2 in DMF, 0.4 ml/hr flow, 15 cm distance, 11kv (b) 20;1 wt% PMMA; Spiro 3 in DMF, 0.4ml/hr flow, 12kv,18cm

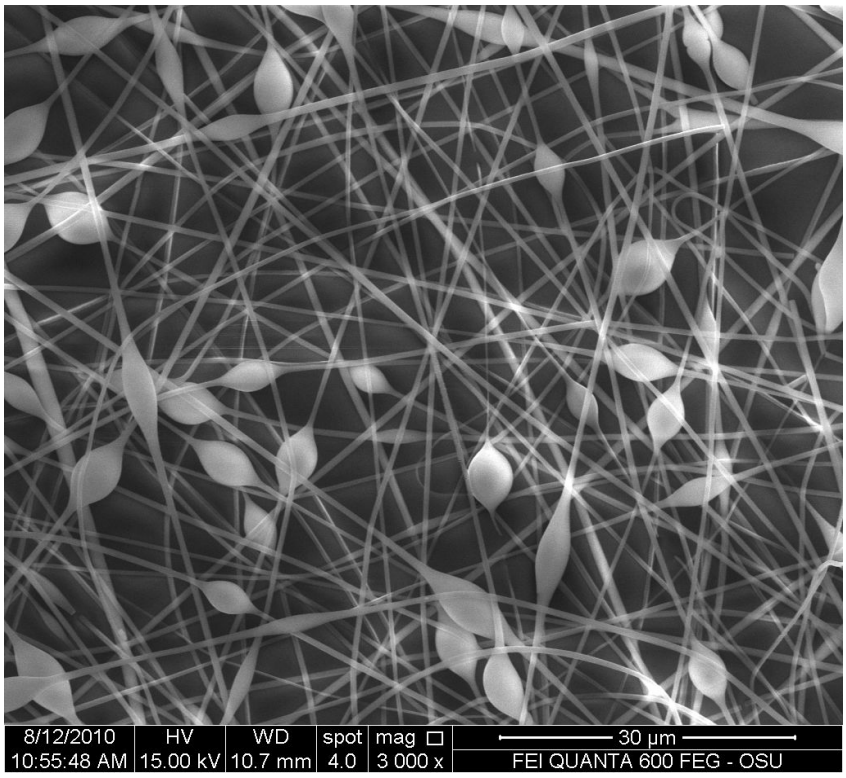

Figure 29: SEM image for a sample based on electrospun parameters of: 20 wt% PMMA, 1 wt% Spiro 3 in chloroform, a 25g needle, a 21cm distance, an 12.5 kV potential, and a 0.4 ml/hr flow rate

Results for Research Phase V: Addition of ethanol to the solvent

For 20 wt% PMMA and 1 wt% of various spiropyran species in DMF with parameter ranges approaching of 11 kV potential, 18 cm point-plate distances, a 27 g needle, and a 0.4 ml/hr flow rate, fibers were obtained without beading. The morphology can be seen in Figure 30.

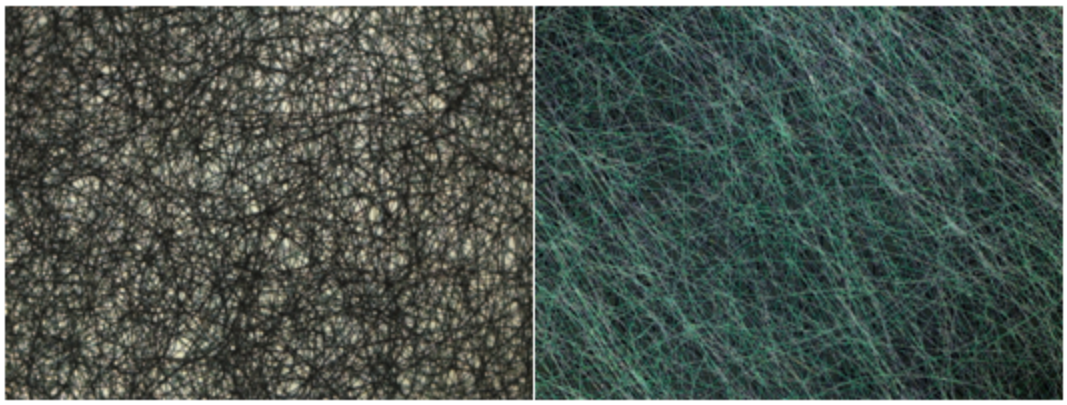

(a) (b)

Figure 30: Microscope images for electrospun samples with parameters of (a) 20 wt% PMMA; 1 wt% Spiro 3 in 3:2 DMF:EtOH, 0.4 ml/hr flow, 18 cm distance, 12kv (b) 20;1 wt% PMMA; Spiro 3 in 3:2 DMF:EtOH, 0.4ml/hr flow, 10kv,18cm

The fibers proved to be photochromic, see Figure 32, Figure 31, and Figure **33**.

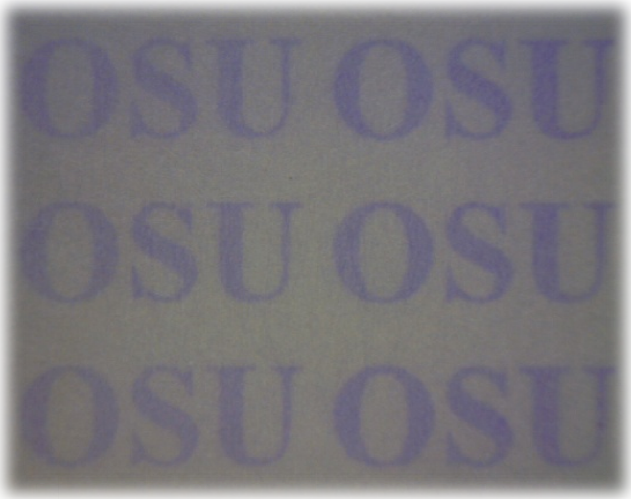

Figure 31: The letters “OSU” have been imprinted into photochromic fibers using and SF 100 as a UV source, Nammoonnoy (*7*).

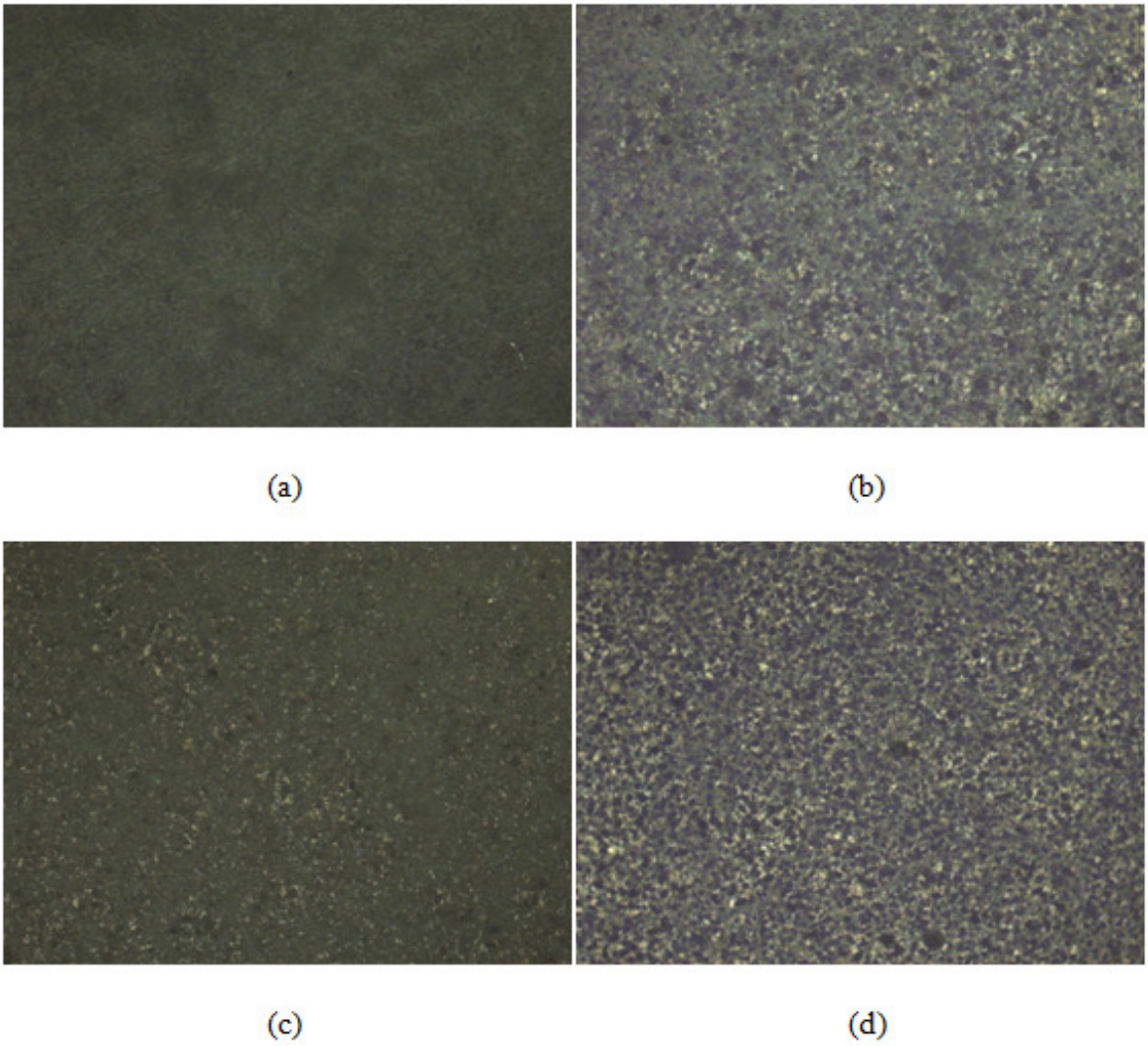

Figure 32: UV tests 0.4ml/hr, 10cm, 17kv,15 wt% PMMA, 1wt% Spiro 3 (a) before UV (b) same place after UV (c) different place before UV (d) same as c after UV

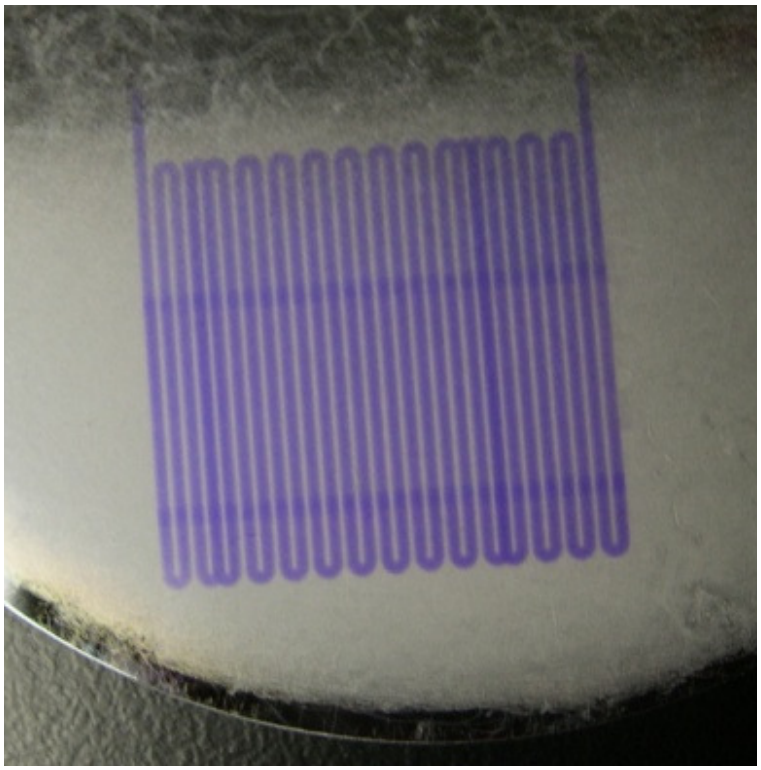

Figure 33: An S-channel, of a type commonly seen in microfluidic applications, has been patterned onto photochromic fibers using the SF 100, Nammoonnoy (*7*).

3.4 Discussion

As was mentioned previously, the results of the electrospinning optimization can be summarized in five major time periods of research. The first time period began when initial parameters were run immediately after the electrospinner was constructed. These parameters being an amalgam of literature values, there was no guarantee that they would work. Typical parameters in these early runs included: 5 wt% PMMA in chloroform, total potentials of 15-20 kV, a point-plate distance of 25cm, and syringe pump flow rates of 0.5-0.75 ml/hr. It seemed that we only got spraying in these early runs. It became apparent based on the literature and our own observations that increasing the

concentration would increase the amount of monomers available to be spun, and would result in actual spinning and not spraying.

When the concentration of polymer in the solution was increased up to 15 wt%, fibers were obtained. But this is when we began to notice the problems (beading and too rapid polymerization) that would inevitably lead to changing the solvent. Even after spiropyran molecules were added to the solution, the beading and rapid polymerization problems persisted. Since it was desired to have small fibers, solutions such as drastically reducing point-plate distance were not considered. Instead, changing to a solvent with a different conductivity was proposed. As can been seen in Table **2**, chloroform has a relatively low boiling point and low conductivity compared to Dimethylformaldahyde, DMF. It was hoped that a higher conductivity solvent would increase the effect of the electrostatic field on the solution, and a solution with a higher boiling point wouldn't vaporize as rapidly, thus allowing for the relatively high distances, high field potentials, and therefore small fibers.

Table 2: Important parameters for solvents used in the electrospinning optimization. Sources: (a) (*21*) (b) (*22*) (c) (*23*)

	Dielectric Constant	BP (°C)	S.G. at 20 °C
Chloroform	4.81 [c, (at 20 °C)]	61.0 [a]	1.489 [a]
DMF	36.71 [c, (at 25 °C)]	153 [b]	0.944 [b]
Ethanol	24.55 [c, (at 25 °C)]	78.5 [a]	0.789 [a]

When the solvent was switched to DMF, spinning was improved (able to get better coverage at these parameters with less clogging and rapid polymerizing). But there was still beading. When ethanol was added to the solution, and the ratio of DMF:EtOH

optimized at 3:2, beading was eliminated. Above all else, what was proven is that the fibers spun were photochromic.

3.5 Conclusion

The task of constructing and optimizing an electrospinner was undertaken. The result were fibers that spin fairly well, have no beading, and when functionalized with spiropyran are photochromic. It remains to be seen the extent to which these fibers can affect the wettability of liquids on their surface. Furthermore, continued optimization is planned to reduce the diameter of the fibers even further.

Conclusion

It has been demonstrated that several species of photochromism, both commercial and functionalized in-lab, are photoswitchable at room temperature. It has been further shown that these spiropyran molecules can be used to functionalize physically modified surfaces as well as electrospun nanofibers. Photoswitchable wettability has been proven in the physically modified surfaces, and photochromism has been proven in the functionalized nanofibers.

Continued optimization of both processes is planned for the future, and it has been shown in this body of work that functionalized surfaces and fibers are possible. It has also been shown that photoswitchable wettability can be performed using only UV irradiation and monochromic visible irradiation, and as such a system of asymmetric lighting should be able to create wettability gradients in surfaces that will lead to photoactuated droplet movement.

Bibliography

1. W. P. Bishop, K. C. Humpherys, P. T. Randtke, Poly (halo) styrene Thin Film Dosimeters for High Doses. *Review of Scientific Instruments* **44**, 443 (1973).
2. Y. Hirshberg, Reversible formation and eradication of colors by irradiation at low temperatures. A photochemical memory model. *Journal of the American Chemical Society* **78**, 2304 (1956).
3. J. H. Day, Thermochromism. *Chemical Reviews* **63**, 65 (1963).
4. E. Fischer, Y. Hirshberg, Formation of coloured forms of spirans by low-temperature irradiation. *J. Chem. Soc* **74**, 4522 (1952).
5. R. Heiligman-Rim, Y. Hirshberg, E. Fischer, PHOTOCHROMISM IN SPIROPYRANS. PART V. 1 ON THE MECHANISM OF PHOTOTRANSFORMATION. *The Journal of Physical Chemistry* **66**, 2470 (1962).
6. S. Wang, Y. Song, L. Jiang, Photoresponsive surfaces with controllable wettability. *Journal of Photochemistry and Photobiology C: Photochemistry Reviews* **8**, 18 (2007).
7. M. T. Koesdjojo, J. Nammoonnoy, R. T. Frederick, V. T. Remcho, Development of Photoactivable Nanofiber Membranes for Fluidic Controls. *Not yet published*, (2011).
8. J. Berthier, *Microdrops and digital microfluidics*. (William Andrew Publishing, 2008).
9. G. M. Whitesides, The origins and the future of microfluidics. *Nature* **442**, 368 (2006).
10. T. M. Squires, S. R. Quake, Microfluidics: Fluid physics at the nanoliter scale. *Reviews of modern physics* **77**, 977 (2005).
11. C. G. Cooney, C. Y. Chen, M. R. Emerling, A. Nadim, J. D. Sterling, Electrowetting droplet microfluidics on a single planar surface. *Microfluidics and Nanofluidics* **2**, 435 (2006).
12. B. Dunfield, Oregon State University (2010).
13. K. Ichimura, S. K. Oh, M. Nakagawa, Light-driven motion of liquids on a photoresponsive surface. *Science* **288**, 1624 (2000).
14. T. Yamamoto, J. Yamamoto, B. I. Lev, H. Yokoyama, Light-induced assembly of tailored droplet arrays in nematic emulsions. *Applied physics letters* **81**, 2187 (2002).
15. A. Diguet *et al.*, Photomanipulation of a Droplet by the Chromocapillary Effect13. *Angewandte Chemie International Edition* **48**, 9281 (2009).
16. J. Nammoonnoy, A photoactivable microfluidic device for heavy metal ion extraction. (2010).
17. B. Sundaray *et al.*, Electrospinning of continuous aligned polymer fibers. *Applied physics letters* **84**, 1222 (2004).
18. T. J. Sill, H. A. von Recum, Electrospinning: applications in drug delivery and tissue engineering. *Biomaterials* **29**, 1989 (2008).
19. J. Deitzel, J. Kleinmeyer, D. Harris, N. Beck Tan, The effect of processing variables on the morphology of electrospun nanofibers and textiles. *Polymer* **42**, 261 (2001).

20. M. Wang *et al.*, Preparation of photochromic poly (vinylidene fluoride-co-hexafluoropropylene) fibers by electrospinning. *Polymer* **50**, 3974 (2009).
21. R. M. Felder, R. Rousseau, *Elementary principles of chemical processes*. (John Wiley & Sons, Inc., United States of America, 2005), vol. Third Edition.
22. MSDS. (Sigma-Aldrich Co., Revision Date 03/30/2011).
23. P. S. Russo. ([Online] http://macro.lsu.edu/HowTo/solvents/Dielectric%20Constant%20.htm), vol. 2011.

Appendix 1: Data for Contact Angle Tests of Posted Chip

Appendix Table 1: Test on Chip #1. Note: Four Repetitions of Data

	After Spiro Treatment						
	Measurement 1	Measurement 2	Measurement 3	Measurement 4	mean	stdev	error
Grid "2"	70.4	68.9	69.7	72.3	70.3	1.5	1.7
Grid "4"	73.8	71.3	79.4	77.6	75.5	3.7	4.3
Grid "6"	70.1	77.7	77.7	77.9	75.9	3.8	4.5

	After UV Irradiation						
	Measurement 1	Measurement 2	Measurement 3	Measurement 4	mean	stdev	error
Grid "2"	55.6	62.3	51.7	56	56.4	4.4	5.2
Grid "4"	49.2	53.8	66.4	62.7	58.0	7.9	9.3
Grid "6"	58.4	69	68.1	60.5	64.0	5.3	6.3

Appendix Table 2: Test on Chip #2. Note: Eight Repetitions of Data

	Before UV Treatment										
	1	2	3	4	5	6	7	8	mean	stdev	error
	[°]	[°]	[°]	[°]	[°]	[°]	[°]	[°]	[°]	[°]	[°]
"Grid 2"	68.3	71.2	78.7	81.8	67.4	70.3	69.2	68.5	71.9	5.0	3.3
"Grid 4"	72.4	68.1	71.7	77.4	74.9	75.7	66.4	66.8	71.7	3.9	2.6
"Grid 6"	76.9	71.6	67.5	73.8	72.9	73.1	62.0	68.6	70.8	4.3	2.9
	After UV Treatment										
	1	2	3	4	5	6	7	8	mean	stdev	error
	[°]	[°]	[°]	[°]	[°]	[°]	[°]	[°]	[°]	[°]	[°]
"Grid 2"	54.2	60.1	72.7	74.1	57.6	57.5	60.8	56.3	61.7	7.0	4.7
"Grid 4"	57.7	57.7	60.9	62.1	66.9	51.7	56.2	60.4	59.2	4.2	2.8
"Grid 6"	61.3	61.7	61.9	57.3	67.4	63.7	58.5	44.6	59.6	6.4	4.3

Appendix 2: ANOVA Analyses

Appendix Table 3: ANOVA analysis on the data from Appendix Table 1

Anova: Single Factor						
SUMMARY						
Groups	*Count*	*Sum*	*Average*	*Variance*		
Before UV	12	886.8	73.9	15.22545455		
After UV	12	713.7	59.475	41.72568182		
ANOVA						
Source of Variation	*SS*	*df*	*MS*	*F*	*P-value*	*F crit*
Between Groups	1248.48375	1	1248.48375	43.84403296	1.17053E-06	4.300949462
Within Groups	626.4625	22	28.47556818			
Total	1874.94625	23				

Appendix Table 4: ANOVA analysis on the data from Appendix Table 2

Anova: Single Factor						
SUMMARY						
Groups	*Count*	*Sum*	*Average*	*Variance*		
Before UV	24	1715.202	71.46675	20.81988098		
After UV	24	1443.454	60.14391667	38.68430678		
ANOVA						
Source of Variation	*SS*	*df*	*MS*	*F*	*P-value*	*F crit*
Between Groups	1538.478656	1	1538.478656	51.70992881	4.71523E-09	4.051748565
Within Groups	1368.596318	46	29.75209388			
Total	2907.074975	47				

Appendix 3: Electrospinner SOP for the Remcho Lab Group

Electrospinning SOP

Created by Ryan Frederick and Brian Fuchs
Last Updated: 12/13/10

Prepare Solution

- Measure out appropriate amount of solvent(s) and place into a vial
- Add polymer solution (e.g. PMMA) in appropriate amount into the solvent
- Mix thoroughly. If necessary take advantage of the 50 °C oven in the corner lab, vortexes, and the vial rotisserie
- When polymer is thoroughly mixed, add functional molecule (e.g. spiropyran) in appropriate amount
- Mix thoroughly again
- If the functional molecule is sensitive to light, wrap vial in Al foil

Set Up

- Plug in the power supplies
- Take a clean mounting substrate (e.g. Si Wafer or Glass Slide) and place in the slot closest to the syringe pump on the surface mount
- Attach wires in the lead from the negative power supply to the back of the mounted substrate using electrical tape (if glass slide or other insulating substance is used tape Al foil on back of slide)
- Draw polymer solution into a syringe
- If a tubing system is not already prepared, thread Teflon tubing through two Upchurch fittings (one for a syringe connection and one for a needle connection)
- Screw appropriate Upchurch fitting on Teflon tubing into the syringe and screw a needle into the Upchurch fitting on the other end of the tube
- Place syringe in the syringe pump
- Take needle and place it on mounting block inside the chamber, mount it using duct tape
- Connect positive high voltage clip onto the needle and aim the needle at the substrate
- Take the end of the exhaust duct and put it into the fume hood

Pump Settings

- Set pump to the diameter of the syringe (e.g. 8.66 mm for 3 mL syringe)
- Set infuse rate to desired flow rate (e.g. 0.4 mL/hr typical)
- Make sure Pump is set to infuse for electrospinning

Electrospinning

- Set power supplies to desired parameters (Negative Supply typically stays maxed out at 3 kV; 8 kV typical on the positive)
- Push solution into the tip of the needle so that the solution just barely starts coming out of the needle and wipe the needle tip dry

- Start the syringe pump
- Close the chamber door and quickly turn on both power supplies (*Note: There is a five second delay on the positive supply)
- Make sure spinning occurs and let the system spin for the desired amount of time or until desired coat is obtained
- Turn off the power supplies
- Plug in the fan and let the system sit for three minutes to allow removal of any nanofibers in the chamber
- Open the chamber door and discharge the needle and the mounting surface with a grounded discharging pole (copper wire threaded through a semi-hollow glass tube)
- Check the back of the mounting substrate and wipe off any polymer fibers stuck to the back
- Remove the mounting surface and stick it face up in a Petri dish
- If the functional molecule is sensitive to light, wrap the dish in Al foil
- Wipe the end of the needle of any excess polymer solution

Things to look for while electrospinning:

- Make sure solution is coming out of the needle
- Make sure solution is spinning fibers
- Solution clogging the needle tip (a little polymer formation at tip can be ok, but eventually it will start interfering with the spinning process)
- Fibers sticking to both the plate and other surfaces inside the chamber (not much can be done to fix this mid run)
- Loose fiber buildup on the mounted substrate

Safety Precautions:

- Use gloves whenever doing anything inside the chamber or doing anything with the solution
- Always let the chamber sit with the fan running before opening the chamber after electrospinning to avoid exposure to nanoparticles and organic solvents
- Make sure power supplies are off before opening the chamber
- Make sure surfaces are discharged before touching any metal in the chamber

Parameters for Optimal Fibers with Aryl Silane Spiropyran:
Optimized: Smallest fibers with no beading as of 8/26/10 Aryl Silane Spiropyran run.

Solution:

- 3:2 DMF:EtOH solution
- 20 wt% PMMA added to solution
- 1 wt% Spiropyran in polymeric solution

Electrospinner:

- 27 gauge needle
- 0.4 mL/hr flow rate on syringe pump

- 18 cm distance between needle tip and wafer

Additional Notes:

- Substrate was three inch, p-type, silicon wafer. Fiber morphology transfers to other substrates (e.g. glass slides) when the same parameters are used, but the coating is small and uneven.
- The ambient temperature was 24 °C; desiccants were present near the site of electrospinning.

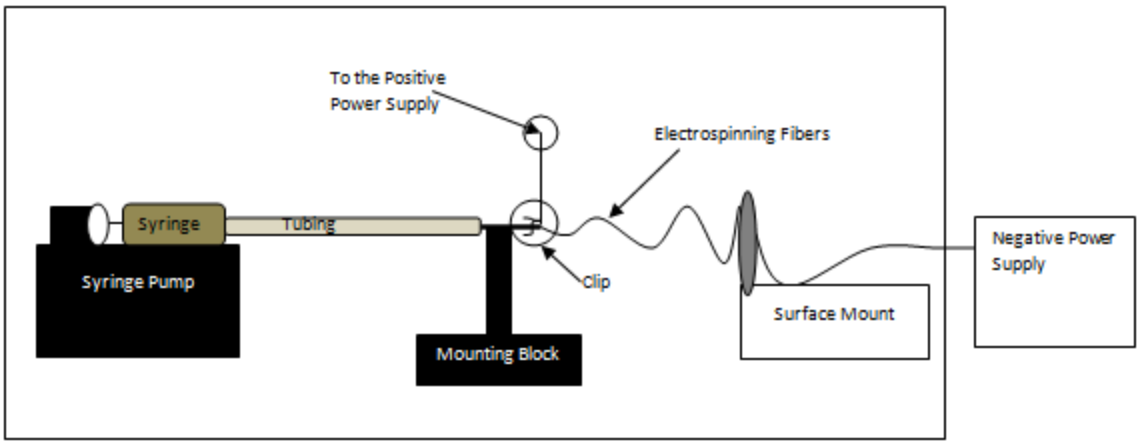

Appendix Figure 1: Schematic that accompanies original SOP for the electrospinner. (Fuchs et al. 2010).